Electronic Supplementary Material (ESI) for ChemComm.

Supporting Information for:

Chiroptical sensing of perrhenate in aqueous media by a chiral organic cage

Riccardo Mobili,[±] Giovanni Preda,[±] Sonia La Cognata, Lucio Toma,

Dario Pasini,* Valeria Amendola,*

Department of Chemistry – University of Pavia Via Taramelli 12 – 27100 Italy

[±] Equal contribution

Table of Contents

1. Materials and Methods

Synthesis. All reagents for syntheses were purchased from Sigma-Aldrich and used without further purification. All reactions were performed under nitrogen. High-resolution mass spectra were recorded on a Sciex X500B QTOF System (Framingham, U.S.A.) operated in the ESI mode. ^{1}H- and ^{13}C-NMR spectra were recorded on a Bruker AVANCEIII 400 MHz (operating at 9.37 T, 400 MHz), equipped with a 5 mm BBO probe head with Z-gradient (Bruker BioSpin) or Bruker AMX 300 MHz. UV−vis spectra were collected using a Varian Cary 50 SCAN spectrophotometer, with quartz cuvettes of the appropriate path length at 25.0 ± 0.1 °C. Emission spectra were collected using a Perkin Elmer LS50B fluorimeter, with a quartz cuvette of 1 cm path length. CD spectra were collected on a JASCO J1500 spectropolarimeter with quartz cuvettes of the appropriate path length at 25.0 ± 0.1 °C. The macrocyclic intermediate **A**, [S1],[S2] (R)-3,3'-diformyl-1,1'-binaphthyl-2,2'-diol **B** and or (R)-3,3'-diformyl-1,1'-binaphthyl-2,2'-dimethylether[S3] **C** were prepared following previously reported syntheses. Characterization data were consistent with the literature.

Molecular Modelling. A theoretical approach was used to give useful suggestions into the conformational preferences of the binaphthyl cages **1** and **2**, and their complexes with perrhenate anion, $[\mathbf{1}H_6(ReO_4)]^{5+}$ and $[\mathbf{2}H_6(ReO_4)]^{5+}$. All the calculations were carried out with the Gaussian 09 program package[S4] within the density functional approach at the B3LYP level with the 6-31G(d) basis set for all atoms except the effective core potential LanL2DZ basis set used for rhenium. The free cages were modeled as hexavalent cations whereas for the perrhenate complexes an overall +5 charge was considered. The solvent effect was taken into account by using a self-consistent reaction field (SCRF) method, based on the polarizable continuum model (PCM), choosing water as the solvent.

Potentiometric titrations. Potentiometric titrations were performed in water-methanol mixtures (35% v/v and 70% v/v for **1** and **2**, respectively) because of the low solubility of both cages in pure aqueous solution. Either $NaNO_3$ or tetrabutylammonium nitrate were employed as supporting

electrolytes at 0.025 M concentration. In a typical experiment, 15 mL of the receptor solution (5×10^{-4} M) was treated with excess HNO_3 (1.0 M). Titrations were performed by addition of 10 μL aliquots of carbonate-free standard 0.1 M NaOH, recording 80−100 points for each titration. Prior to each potentiometric titration, the standard electrochemical potential (E°) of the glass electrode was determined in the proper solvent mixture by a titration experiment according to the Gran method. Protonation titration data (emf vs mL of NaOH) were processed with the HyperQuad package[S5] to estimate the equilibrium constants. For both cages, six protonation equilibria were observed and the corresponding constants are reported in Table S1. For the purpose of our study, it should be noted that, at pH 2, the main species in solution are the hexaprotonated forms of **1** and **2**, presenting all the secondary amino groups protonated. We can consider that H_6L^{6+} is the main species at pH 2 also in 100% H_2O (i.e. the medium used for investigations with anions), as already observed by our group in previous studies on bistren azacryptands[S1],[S6]. Unfortunately, all attempts to use 100% H_2O for the potentiometric titrations were unsuccessful because of the precipitation of the cages above pH 4.

Spectrophotometric, spectrofluorimetric and CD titrations. All titrations were performed in aqueous solution (0.05 M CF_3SO_3Na) at 25 °C and inert atmosphere, the pH of the solution was set to 2 by addition of concentrated CF_3SO_3H. For the determination of binding constants, receptor solutions were titrated with 1000-fold more concentrated solutions of the anions as sodium salts. After each addition of sub-stoichiometric amount of the anion, spectra were recorded using quarts cuvettes (UV-vis. and CD, path length: 0.1 cm; fluorimetry, path length: 1 cm). Titration data were processed with the Hyperquad package[S5] to determine the equilibrium constants.

^{1}H-NMR titrations. All measurements were performed at 25 °C in a solution of D_2O (0.05 M CF_3SO_3Na), the pD of the solution was set to 2 by addition of concentrated CF_3SO_3H in D_2O. For the determination of binding constants, receptor was titrated with a 15-fold more concentrate solution of the anion. After each addition of sub-stoichiometric amount of the anion in the NMR

tube containing 0.75 mL of receptor solution, ^{1}H-NMR spectra were recorded. Titration data were processed with HypNMR (Hyperquad package) [S5] to determine the equilibrium constants.

2. Synthetic procedures

Synthesis of 1 and 2

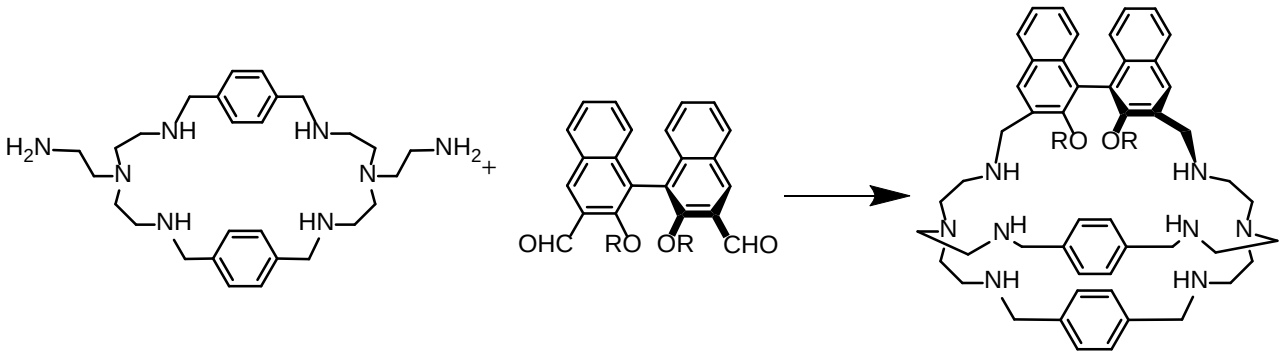

A

B: R = -H
C: R = -Me

1: R = -H
2: R = -Me

Scheme S1

Compound 1. A solution of (*R*)-2,2′-dihydroxy-1,1′-binaphthyl-3,3′-dicarbaldehyde **B** (0.070 g; 0.205 mmol; 1.0 equiv) in MeOH (50 mL) was slowly added dropwise under N_2 to a solution of the macrocyclic intermediate **A** (0.102 g; 0.205 mmol; 1.0 equiv) dissolved in MeOH (100 mL), with continuous magnetic stirring at room temperature. The reaction mixture was stirred at room temperature under N_2 overnight. The solution was filtered to remove insoluble byproducts and then heated to reflux. $NaBH_4$ (0.155 g; 4.1 mmol; 20 equiv) was added in small portions in order to reduce imine bonds. After 12 h the mixture was cooled to room temperature and the solvent was evaporated under vacuum to give a white solid that was dissolved with brine (50 mL) and extracted with DCM (5 × 30 mL). The collected organic phases were then dried (Na_2SO_4), filtered and the solvent was evaporated under vacuum to obtain a dense brown oil (0.19 g) that was immediately purified by precipitation as the nitrate salt as follows: the free cage was dissolved in the minimum amount of EtOH and treated with HNO_3 until precipitation of a solid. The solid was filtered and washed with EtOH and Et_2O. The free cage was then reobtained by dissolving the nitrate salt in basic water and extracting the aqueous mixture with DCM (6 × 25 mL). The collected organic phases, containing the cage, were then dried (Na_2SO_4) and evaporated under vacuum to yield **1** as a

red solid (0.10 g, 60%). ^{1}H-NMR (400 MHz, D_2O + excess CF_3SO_3H) δ: 8.22 (s, 2H, H_4), 7.95 (d, 2H, H_5), 7.24-7.37 (m, 4H, H_{6+7}), 7.00-7.07 (m, 6H, H_{8+ph}), 6.86 (d, 4H, H_{ph}), 4.40+4.71 (m, 4H, H_9), 3.74-4.21 (m, 8H, H_{10+11}), 2.66-3.43 (m, 24H, N-(CH_2-CH_2-N)$_3$); ^{13}C-NMR (100 MHz, D_2O + excess CF_3SO_3H) δ: 43.93, 44.26, 44.73, 47.93, 48.90, 49.62, 50.00, 50.34, 50.62, 114.09, 120.18, 123.99, 124.96, 128.51, 128.74, 130.07, 130.20, 131.09, 131.21, 133.88, 134.44, 151.77; HRMS-ESI (CH_3CN) *m/z*: $[M + H]^+$ calculated for $C_{50}H_{62}N_8O_2$, 807.5068, found 807.5055.

Compound 2. A solution of (*R*)-2,2′-dimethoxy-1,1′-binaphthyl-3,3′-dicarbaldehyde **C** (0.060 g; 0.162 mmol; 1.0 equiv) in MeOH (50 mL) was slowly added dropwise under N_2 to a solution of the macrocyclic intermediate **A** (0.081 g; 0.162 mmol; 1.0 equiv) dissolved in MeOH (70 mL) with continuous magnetic stirring. The reaction mixture was stirred under N_2 at room temperature overnight. The MeOH solution was filtered to remove insoluble byproduct and then heated to reflux. $NaBH_4$ (0.130 g; 3.24 mmol; 20 equiv) was added in small portions in order to reduce imine bonds. After 12 h, the mixture was cooled to room temperature and the solvent was evaporated under vacuum to give a white solid that was dissolved with brine (30 mL) and extracted with DCM (5 × 20 mL). The collected organic phases were dried (Na_2SO_4), filtered and the solvent was evaporated under vacuum to obtain a dense brown oil (0.15 g) that was immediately purified by precipitation of the nitrate salt as follows: the free cage was dissolved in the minimal amount of EtOH and treated with HNO_3 until precipitation of a solid. The solid was filtered and washed with EtOH and Et_2O. The free cage was then reobtained by dissolving the nitrate salt in basic water and extracting the aqueous mixture with DCM (6 × 25 mL). The collected organic phases, containing the cage, were then dried (Na_2SO_4) and evaporated under vacuum to yield **2** as a yellow solid (0.07 g, 52%). ^{1}H-NMR (300 MHz, D_2O + excess CF_3SO_3H) δ: 8.16 (s, 2H, H_4), 7.92 (d, 2H, H_5), 6.91-7.45 (m, 10H, $H_{6+7+8+ph}$), 6.83 (d, 4H, H_{ph}), 4.29-4.59 (m, 4H, H_9), 3.75-4.16 (m, 8H, H_{10+11}), 3.13 (s, 6H, H_{12}), 2.47-3.03(m, 24H, N-(CH_2-CH_2-N)$_3$); ^{13}C-NMR (100 MHz, D_2O + excess CF_3SO_3H) δ: 44.16, 44.36, 44.54, 44.74, 47.93, 49.34, 49.71, 50.52, 50.64, 60.94, 123.46, 123.54, 123.67,

125.58, 126.38, 128.50, 129.98, 130.24, 131.22, 131.77, 133.17, 135.04, 154.32; HRMS-ESI (CH_3CN) *m/z*: $[M + H]^+$ calculated for $C_{52}H_{66}N_8O_2$, 835.5381, found 835.5382.

3. Computational studies

For the free cages, due to their high flexibility, a number of different conformers were located for both of them. The two most stable conformers of each compound are reported in Figure S1.

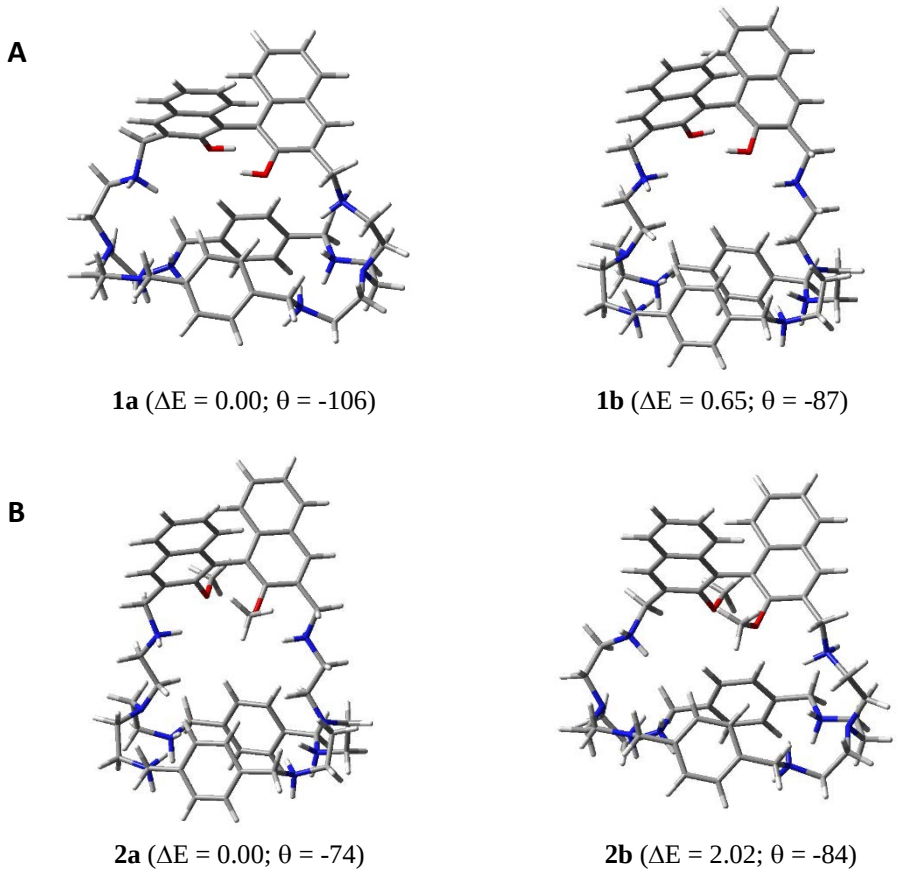

1a (ΔE = 0.00; θ = -106) **1b** (ΔE = 0.65; θ = -87)

2a (ΔE = 0.00; θ = -74) **2b** (ΔE = 2.02; θ = -84)

Figure S1. Three-dimensional plots of the preferred conformers of cages **1** and **2** in their hexaprotonated forms (see **A** and **B** respectively). In parentheses the relative energy ΔE (kcal/mol) and the dihedral angle $\theta_{2\text{-}1\text{-}1'\text{-}2'}$ (°).

The global minima of the two hexaprotonated cages (i.e. $[\mathbf{1}H_6]^{6+}$ and $[\mathbf{2}H_6]^{6+}$) are quite different; **1a** is more compact while **2a** is more elongated with the binaphthyl moiety positioned apart from the remaining portion of the structure. Moreover, the angle between the planes of the naphthyls is about 30 degrees larger in the case of **1a** with respect to **2a**. It is worthy pointing out the similarity between conformer **2b** and conformer **1a** as well as that of **1b** with **2a**. Though the two most stable conformer of each cage show a similar geometry, the stability order is reversed.

Also for the perrhenate complexes $[\mathbf{1}H_6(ReO_4)]^{5+}$ and $[\mathbf{2}H_6(ReO_4)]^{5+}$ a lot of conformers were found, the three most stable being reported in Figure S2. The perrhenate anion is well hosted by conformer **1a** with the two naphthyl hydroxyl groups hydrogen-bonded to two distinct perrhenate

oxygen atoms, in addition to several H-bonds involving the cationic NH_2 groups. Conversely, in the case of the cage **2** the binaphthyl moiety does not give any contribution to the complexation of perrhenate, which, in the preferred conformer $[\mathbf{2b}H_6(ReO_4)]^{5+}$, lies on the lower side of the cage.

A

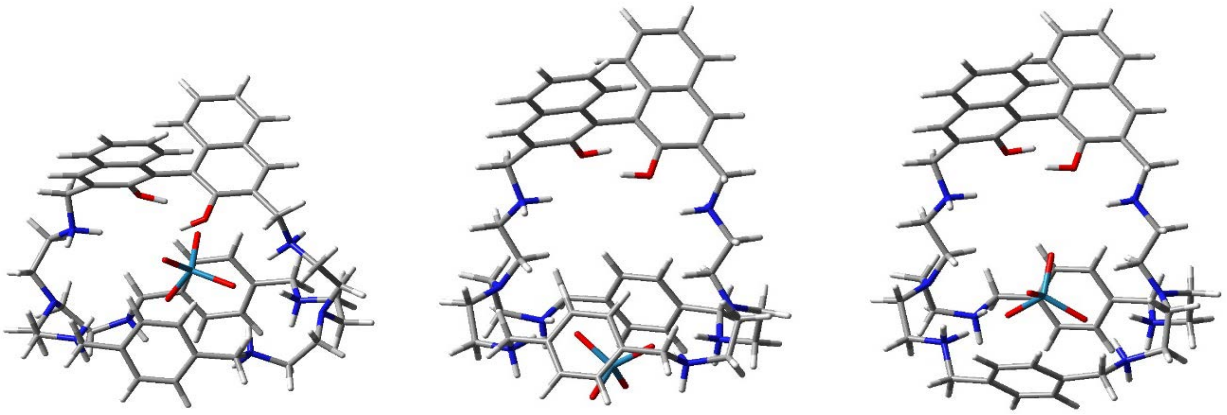

$[\mathbf{1a}H_6(ReO_4)]^{5+}$ (ΔE = 0.00; θ = -111) $[\mathbf{1b}H_6(ReO_4)]^{5+}$ (ΔE = 1.99; θ = -85) $[\mathbf{1c}H_6(ReO_4)]^{5+}$ (ΔE = 3.00; θ = -88)

B

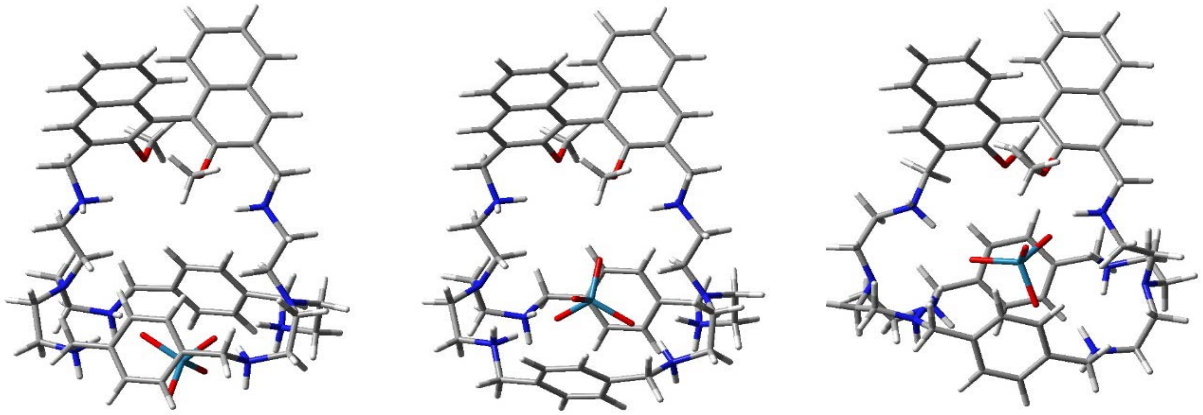

$[\mathbf{2a}H_6(ReO_4)]^{5+}$ (ΔE = 0.00; θ = -75) $[\mathbf{2b}H_6(ReO_4)]^{5+}$ (ΔE = 1.31; θ = -76) $[\mathbf{2c}H_6(ReO_4)]^{5+}$ (ΔE = 1.57; θ = -70)

Figure S2. Three-dimensional plots of the preferred conformers of $[\mathbf{1}H_6(ReO_4)]^{5+}$ (**A**) and $[\mathbf{2}H_6(ReO_4)]^{5+}$ (**B**). In parentheses the relative energy ΔE (kcal/mol) and the dihedral angle $\theta_{2\text{-}1\text{-}1'\text{-}2'}$ (°).

4. Potentiometric titrations

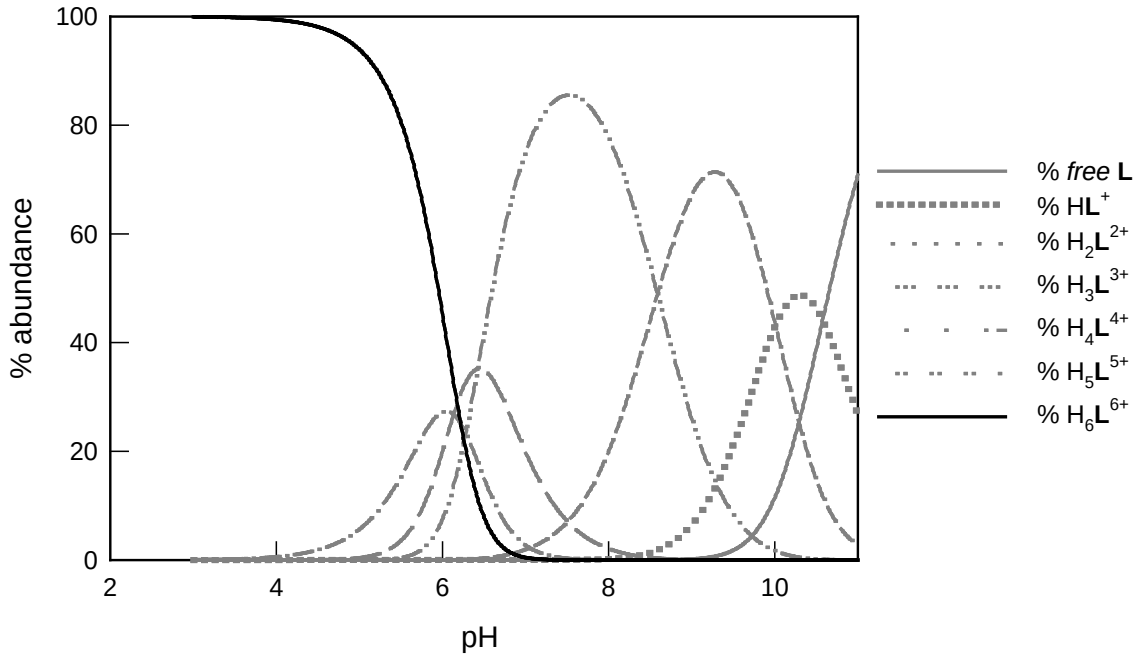

Figure S3. Distribution diagram of the species (% abundance vs. pH) of **1** in H_2O:MeOH (65:35 v:v), 0.025 M $NaNO_3$; T = 25 °C. The corresponding protonation constants are reported in Table S1.

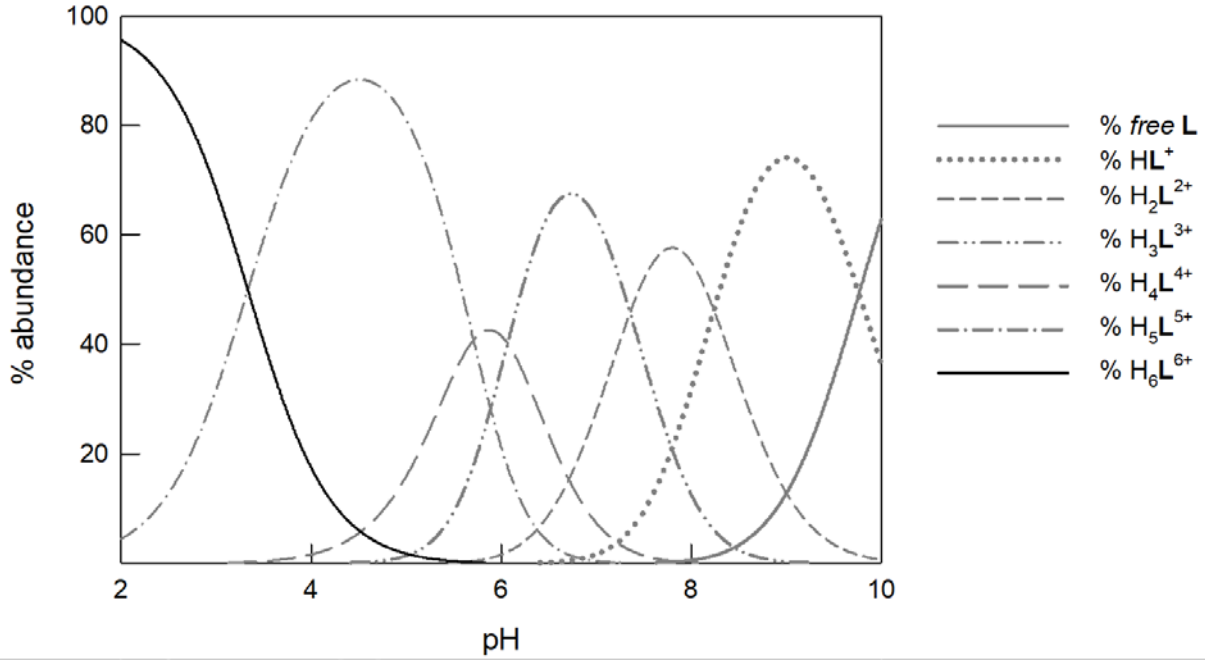

Figure S4. Distribution diagram of the species (% abundance vs. pH) of **2** in H_2O:MeOH (30:70 v:v), 0.025 M tetrabutylammonium nitrate; T = 25 °C. The corresponding protonation constants are reported in Table S1.

Table S1. Protonation constants obtained through potentiometric titrations at 25 °C in H_2O:MeOH mixtures *(a)* 65:35 v:v, 0.025 M $NaNO_3$, *(b)* 30:70 v:v, 0.025 M tetrabutylammonium nitrate.

(a) CAGE **1**	Logβ
$\mathbf{L} + H^+ = H\mathbf{L}^+$	10.57(1)
$\mathbf{L} + 2\ H^+ = H_2\mathbf{L}^{2+}$	20.58(2)
$\mathbf{L} + 3\ H^+ = H_3\mathbf{L}^{3+}$	29.17(2)
$\mathbf{L} + 4\ H^+ = H_4\mathbf{L}^{4+}$	35.60(3)
$\mathbf{L} + 5\ H^+ = H_5\mathbf{L}^{5+}$	41.73(4)
$\mathbf{L} + 6\ H^+ = H_6\mathbf{L}^{6+}$	47.95(4)
(b) CAGE **2**	Logβ
$\mathbf{L} + H^+ = H\mathbf{L}^+$	9.77(2)
$\mathbf{L} + 2\ H^+ = H_2\mathbf{L}^{2+}$	18.01(3)
$\mathbf{L} + 3\ H^+ = H_3\mathbf{L}^{3+}$	25.36(3)
$\mathbf{L} + 4\ H^+ = H_4\mathbf{L}^{4+}$	31.43(4)
$\mathbf{L} + 5\ H^+ = H_5\mathbf{L}^{5+}$	37.14(4)
$\mathbf{L} + 6\ H^+ = H_6\mathbf{L}^{6+}$	40.47(3)

5. UV-Vis. titrations

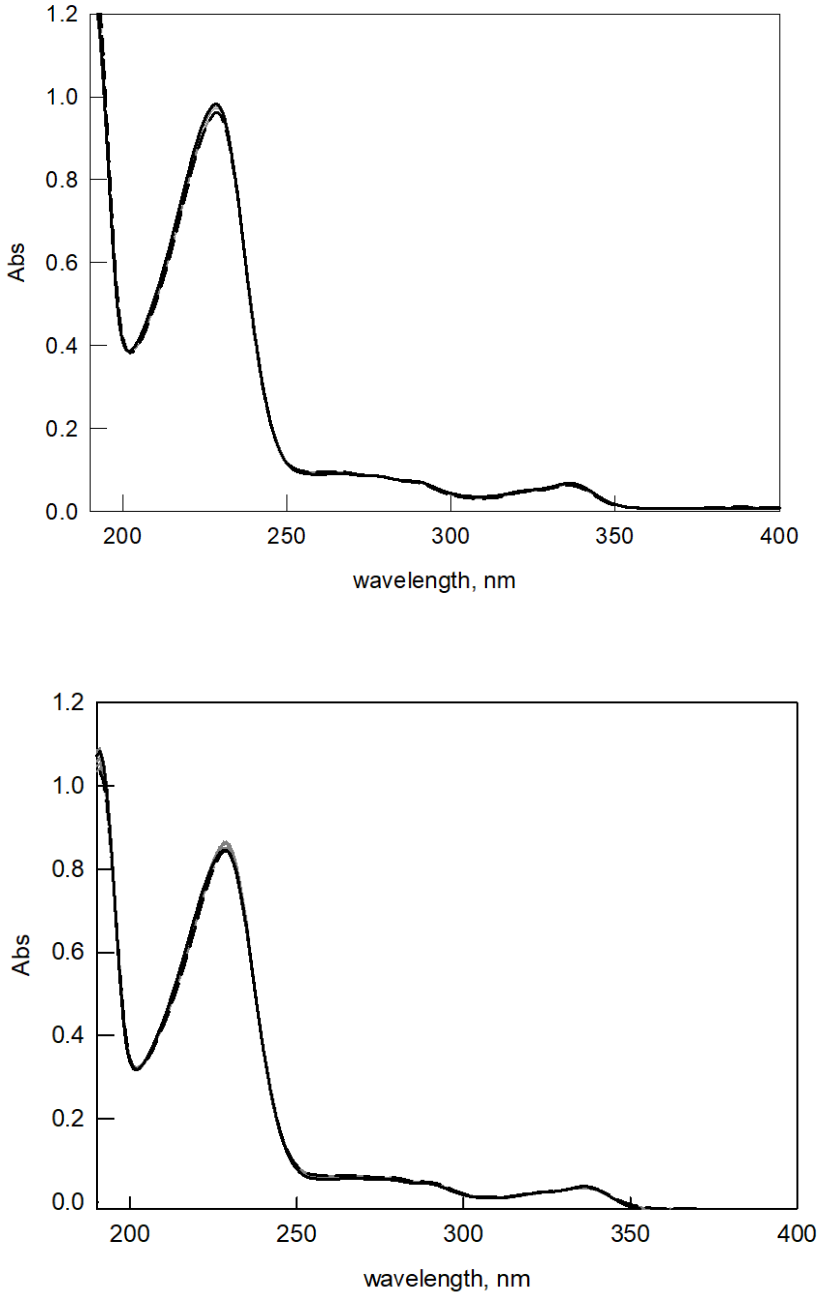

Figure S5. UV-vis. spectra recorded over the titration of an aqueous solution of $[\mathbf{1}H_6]^{6+}$ (0.1 mM, path length = 0.1 cm) with NaCl (top) and Na_2SO_4 (bottom) at pH=2. Solid and dashed lines: initial and final spectra, respectively.

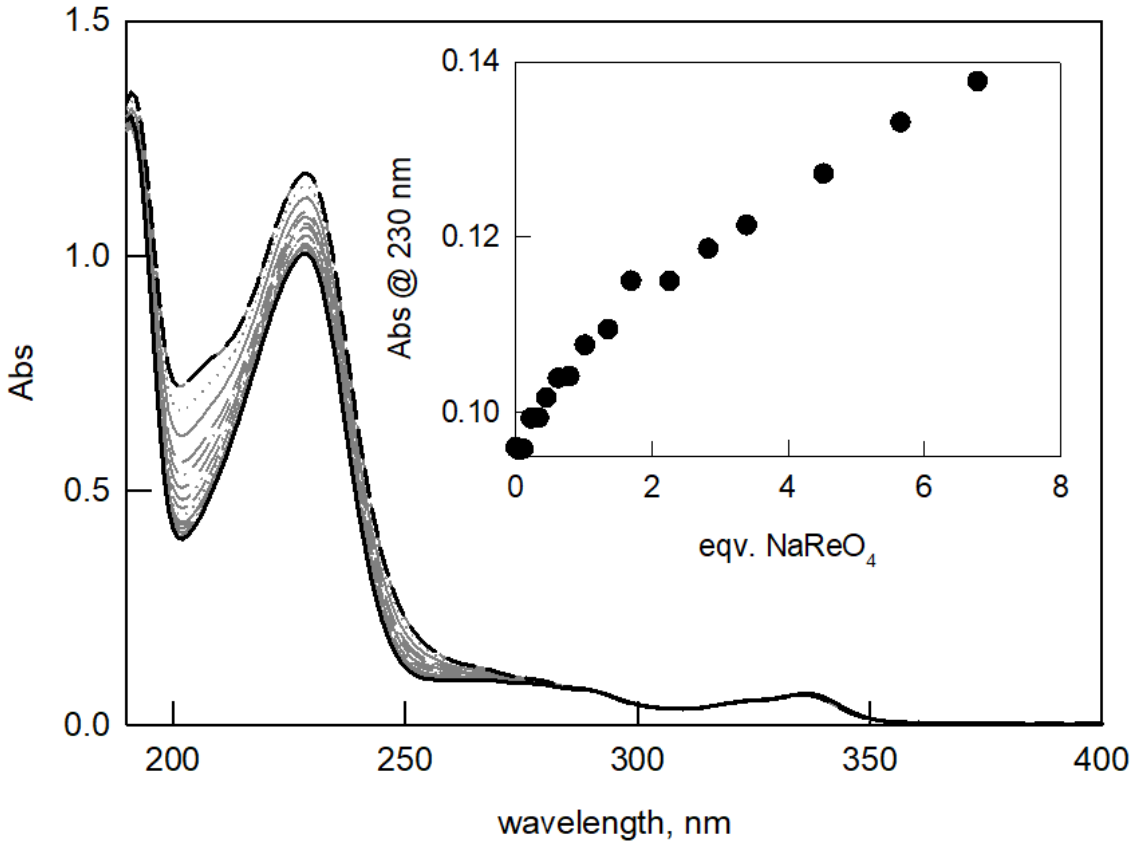

Figure S6. UV-vis. spectra recorded over the titration of an aqueous solution of $[\mathbf{1}H_6]^{6+}$ (0.1 mM, path length = 0.1 cm) with $NaReO_4$ at pH=2. Solid and dashed lines: initial and final spectra, respectively.

6. CD titrations

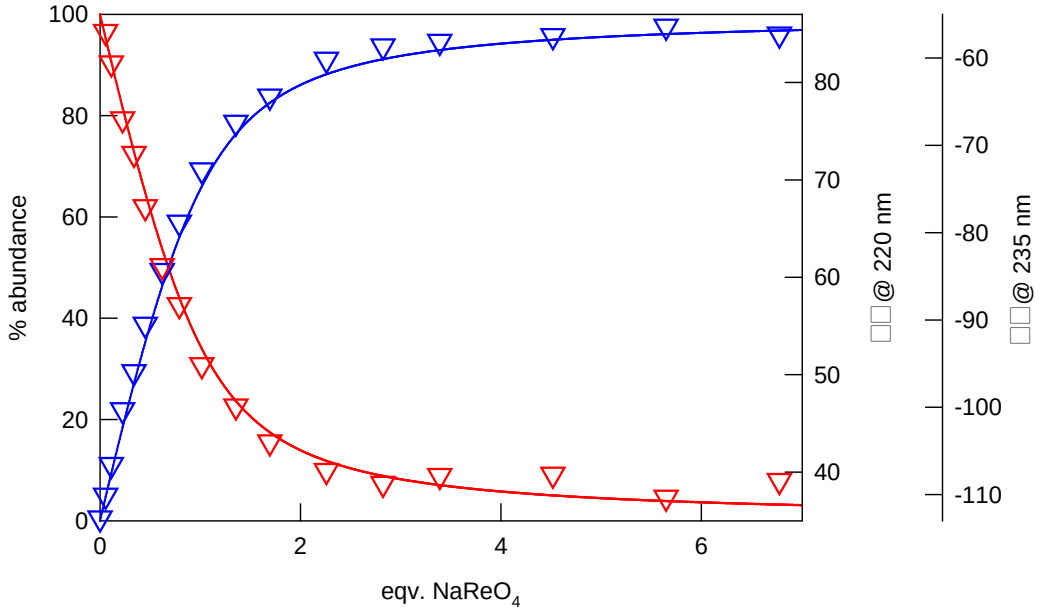

Figure S7. CD titration of $[\mathbf{1}H_6]^{6+}$ with $NaReO_4$ in aqueous solution at pH 2. Distribution diagram of the species (red line: % free $[\mathbf{1}H_6]^{6+}$; blue line: % $[\mathbf{1}H_6(ReO_4)]^{5+}$), superimposed to the experimental profiles of $\Delta\varepsilon$ (M^{-1} cm^{-1}) *vs.* equivalents of $NaReO_4$. Blue and red symbols: experimental profiles of $\Delta\varepsilon$, taken at 220 and 235 nm, respectively.

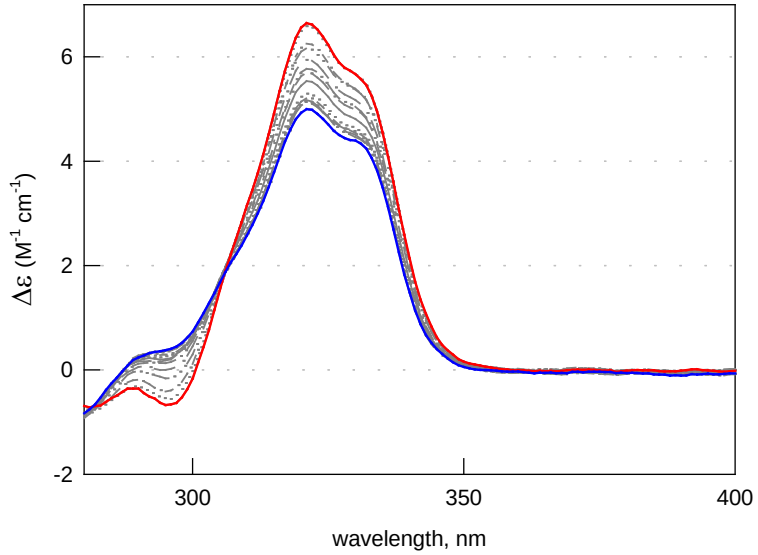

Figure S8. Partial CD spectra (recorded between 280 and 400 nm) taken over titration of $[\mathbf{1}H_6]^{6+}$ (0.1 mM) with $NaReO_4$ in aqueous solution at pH 2 (path length = 1 cm); red and blue lines correspond to the initial and final spectra, respectively.

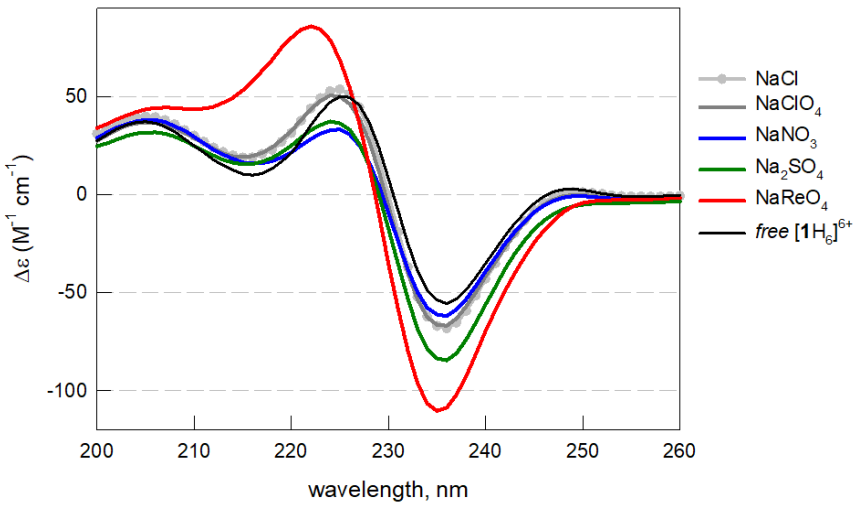

Figure S9. CD spectra taken on $[\mathbf{1}H_6]^{6+}$ in aqueous solution at pH 2 (0.1 mM) and in presence of 5 eqv. sodium salts.

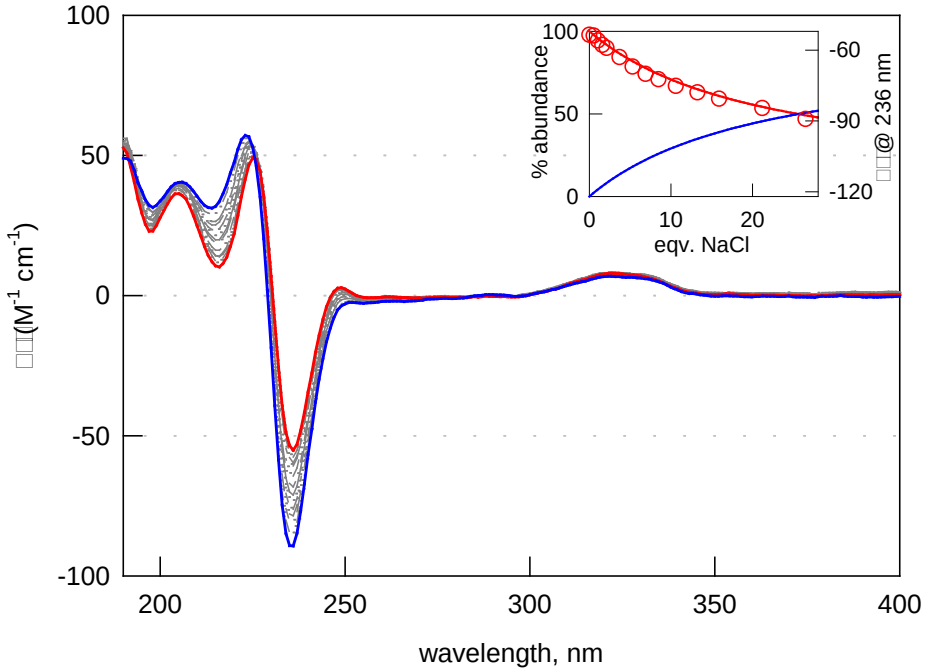

Figure S10. CD spectra taken over the titration of $[\mathbf{1}H_6]^{6+}$ (0.1 mM) with NaCl in aqueous solution at pH 2; red and blue lines correspond to the initial and final spectra, respectively. Inset: distribution diagram of the species (red line: % free of $[\mathbf{1}H_6]^{6+}$; blue line: % of $[\mathbf{1}H_6(Cl)]^{5+}$), superimposed to the experimental profile of $\Delta\varepsilon$ (M^{-1} cm^{-1}) at 236 nm *vs.* equivalents of NaCl.

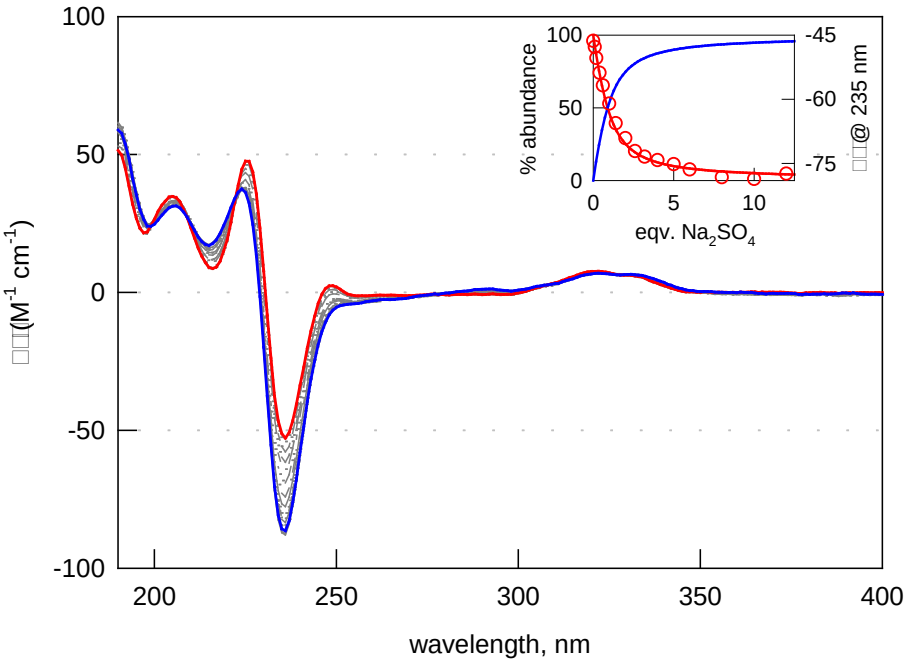

Figure S11. CD spectra taken over the titration of $[\mathbf{1}H_6]^{6+}$ (0.1 mM) with Na_2SO_4 in aqueous solution at pH 2; red and blue lines correspond to the initial and final spectra, respectively. Inset: distribution diagram of the species (red line: % free $[\mathbf{1}H_6]^{6+}$; blue line: % $[\mathbf{1}H_6(SO_4)]^{4+}$), superimposed to the experimental profile of Δε (M^{-1} cm^{-1}) at 236 nm *vs.* equivalents of Na_2SO_4.

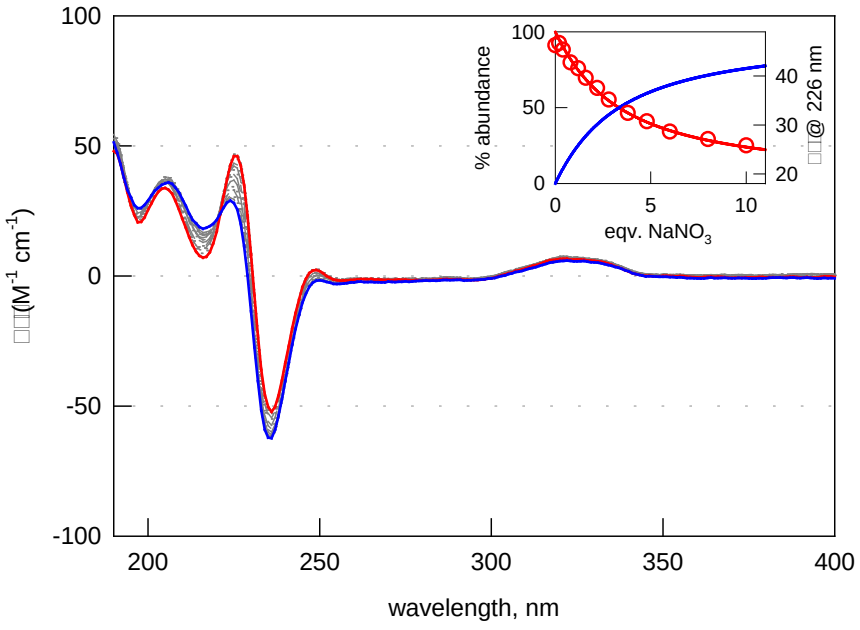

Figure S12. CD spectra taken over the titration of $[\mathbf{1}H_6]^{6+}$ (0.1 mM) with $NaNO_3$ in aqueous solution at pH 2; red and blue lines correspond to the initial and final spectra, respectively. Inset: distribution diagram of the species (red line: % free $[\mathbf{1}H_6]^{6+}$; blue line: % $[\mathbf{1}H_6(NO_3)]^{5+}$), superimposed to the experimental profile of Δε (M^{-1} cm^{-1}) at 226 nm *vs.* equivalents of $NaNO_3$.

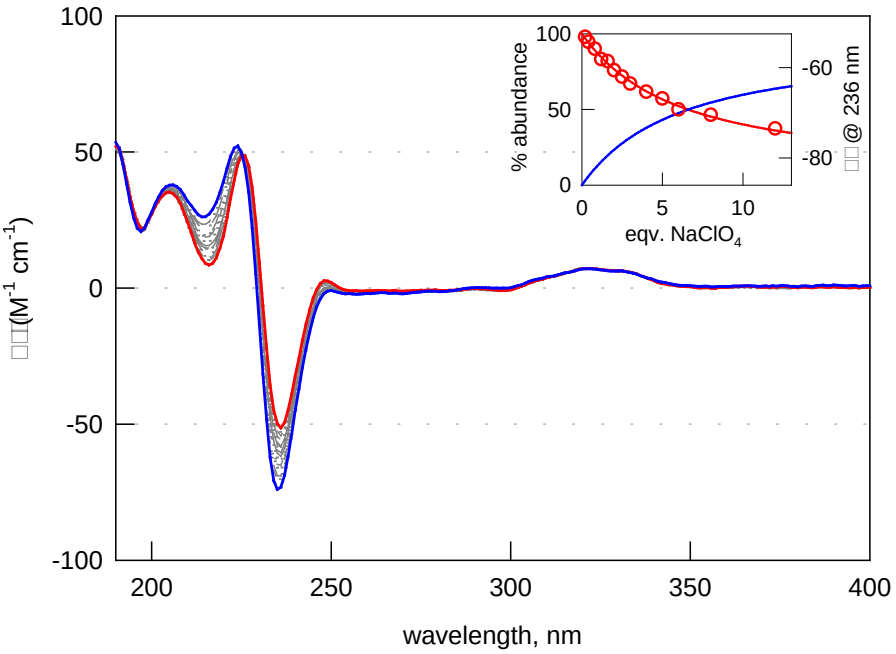

Figure S13. CD spectra taken over the titration of $[\mathbf{1}H_6]^{6+}$ (0.1 mM) with $NaClO_4$ in aqueous solution at pH 2; red and blue lines correspond to the initial and final spectra, respectively. Inset: distribution diagram of the species (red line: % free $[\mathbf{1}H_6]^{6+}$; blue line: % $[\mathbf{1}H_6(ClO_4)]^{5+}$), superimposed to the experimental profile of Δε (M^{-1} cm^{-1}) at 236 nm *vs.* equivalents of $NaClO_4$.

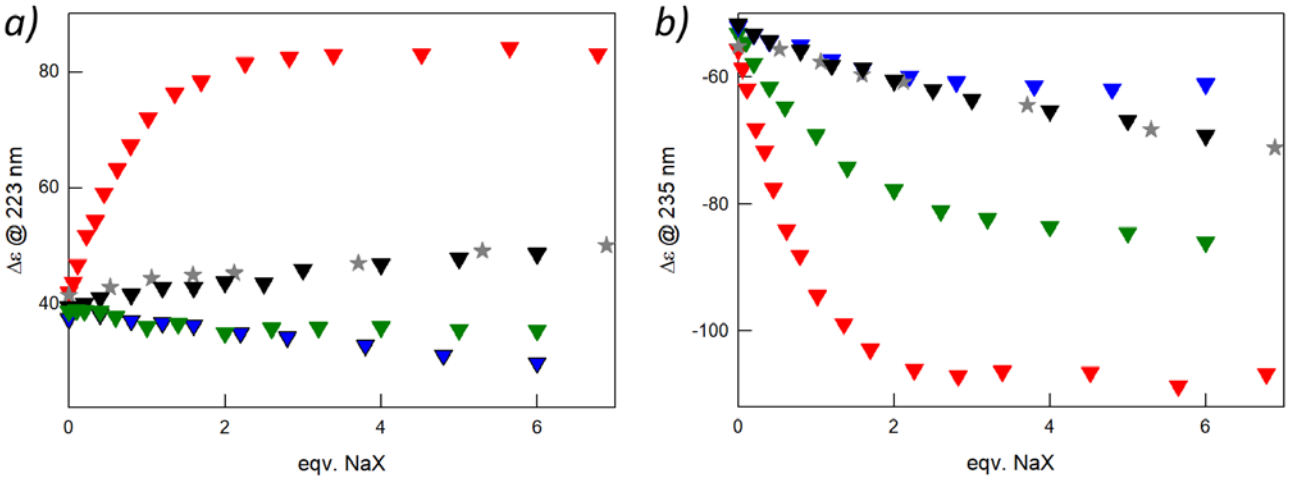

Figure S14. Experimental titration profiles of Δε (M^{-1} cm^{-1}) at 223 and 235 nm (see a) and b), respectively) *vs.* equivalents of the added NaX. The profiles were obtained from the CD titrations on $[\mathbf{1}H_6]^{6+}$ (0.1 mM) with solutions of different sodium salts (symbols: red, $NaReO_4$; blue, $NaNO_3$; green, Na_2SO_4; black triangles, $NaClO_4$; grey stars, NaCl).

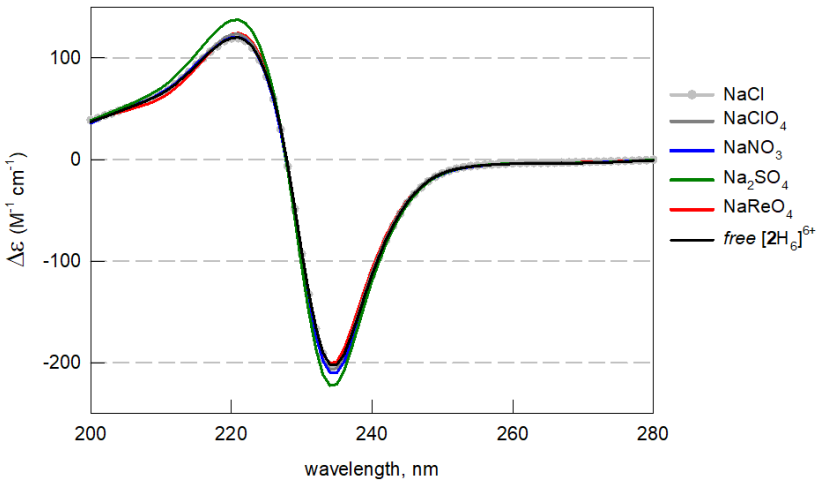

Figure S15. CD spectra taken on $[\mathbf{2}H_6]^{6+}$ in aqueous solution at pH 2 (0.1 mM) alone and in presence of 10 eqv. sodium salts.

7. ^{1}H-NMR titrations

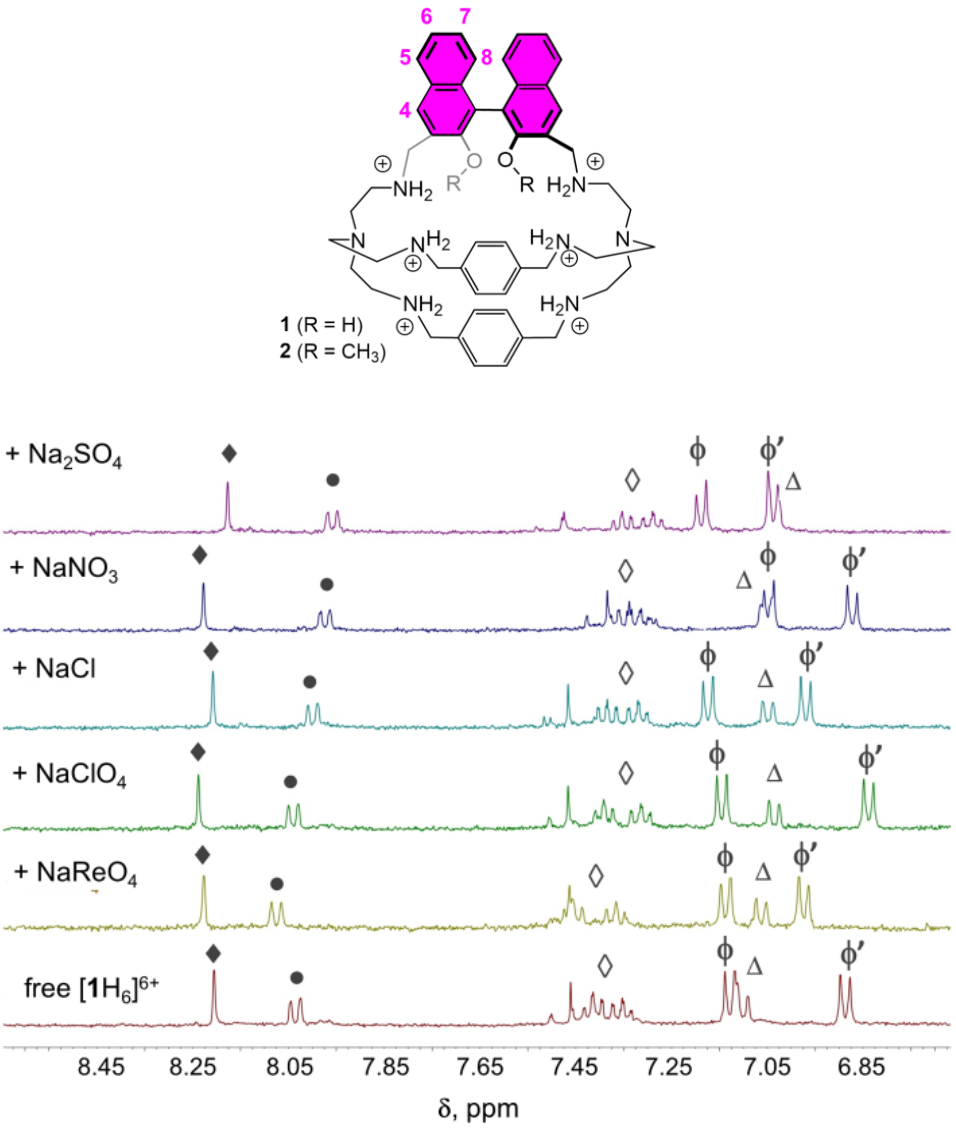

Figure S16. Details of the aromatic regions of the ^{1}H-NMR spectra of $[\mathbf{1}H_6]^{6+}$ (0.6 mM) in D_2O (CF_3SO_3Na 0.05M, pD = 2), before (red line) and after the addition of excess anions (~80 eqv.) as sodium salts (symbols ♦: H4; •: H5; ◊: H6-H7; ϕ, ϕ': phenyl protons; Δ: H8).

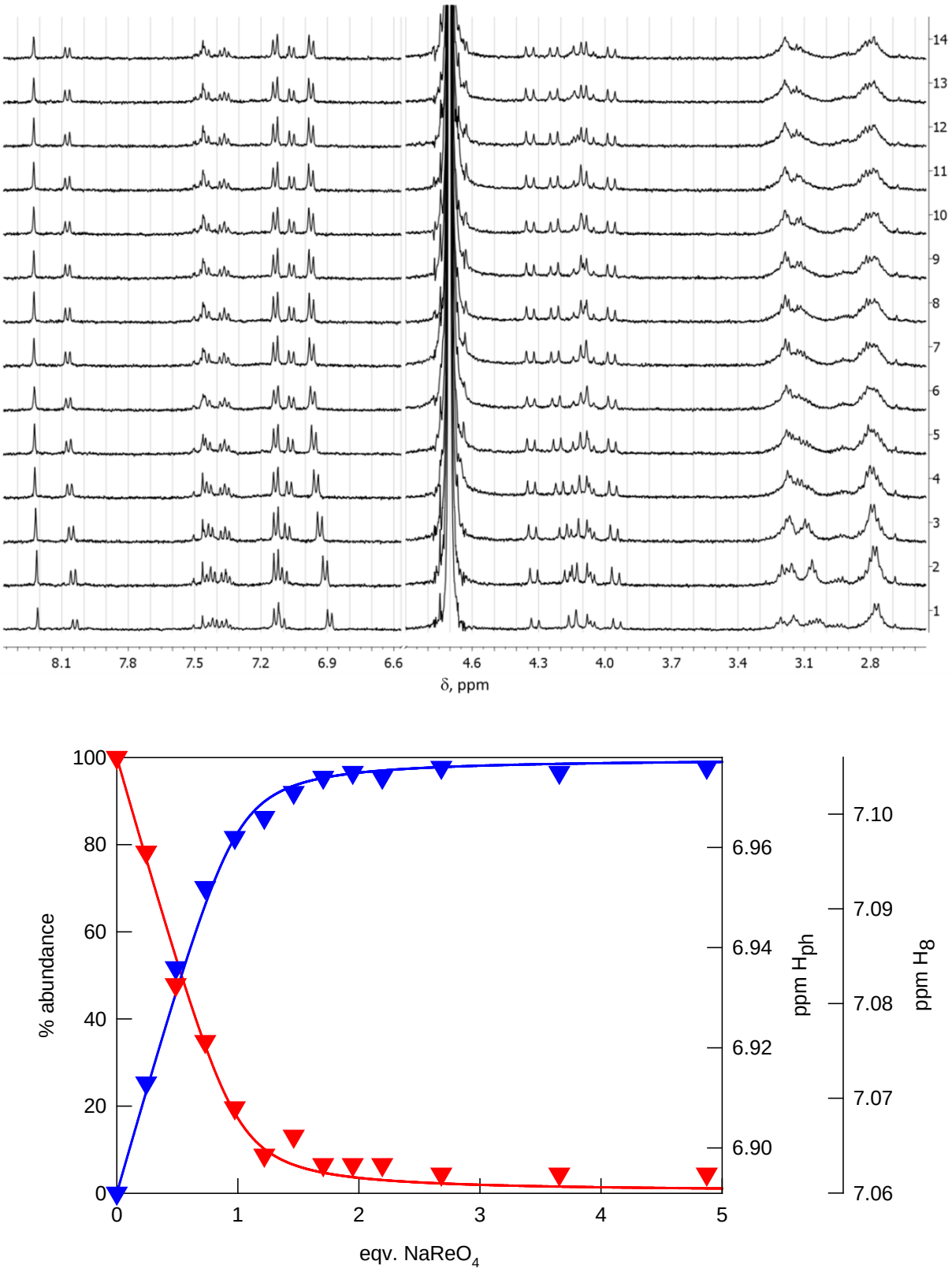

Figure S17. top: family of ^{1}H-NMR spectra taken over the course of the titration of $[\mathbf{1}H_6]^{6+}$ (0.6 mM in D_2O (pD = 2, CF_3SO_3Na 0.05M) with a standard solution of $NaReO_4$, spectrum 1 corresponds to the free receptor; bottom: experimental profiles (chemical shifts of H_{ph} and H_8: blue and red symbols, respectively) superimposed to the distribution diagram of the species *vs.* equivalents of the added sodium salt ($LogK_{11}$ = 4.77). red line = % free $[\mathbf{1}H_6]^{6+}$, blue line = % $[\mathbf{1}H_6(ReO_4)]^{5+}$

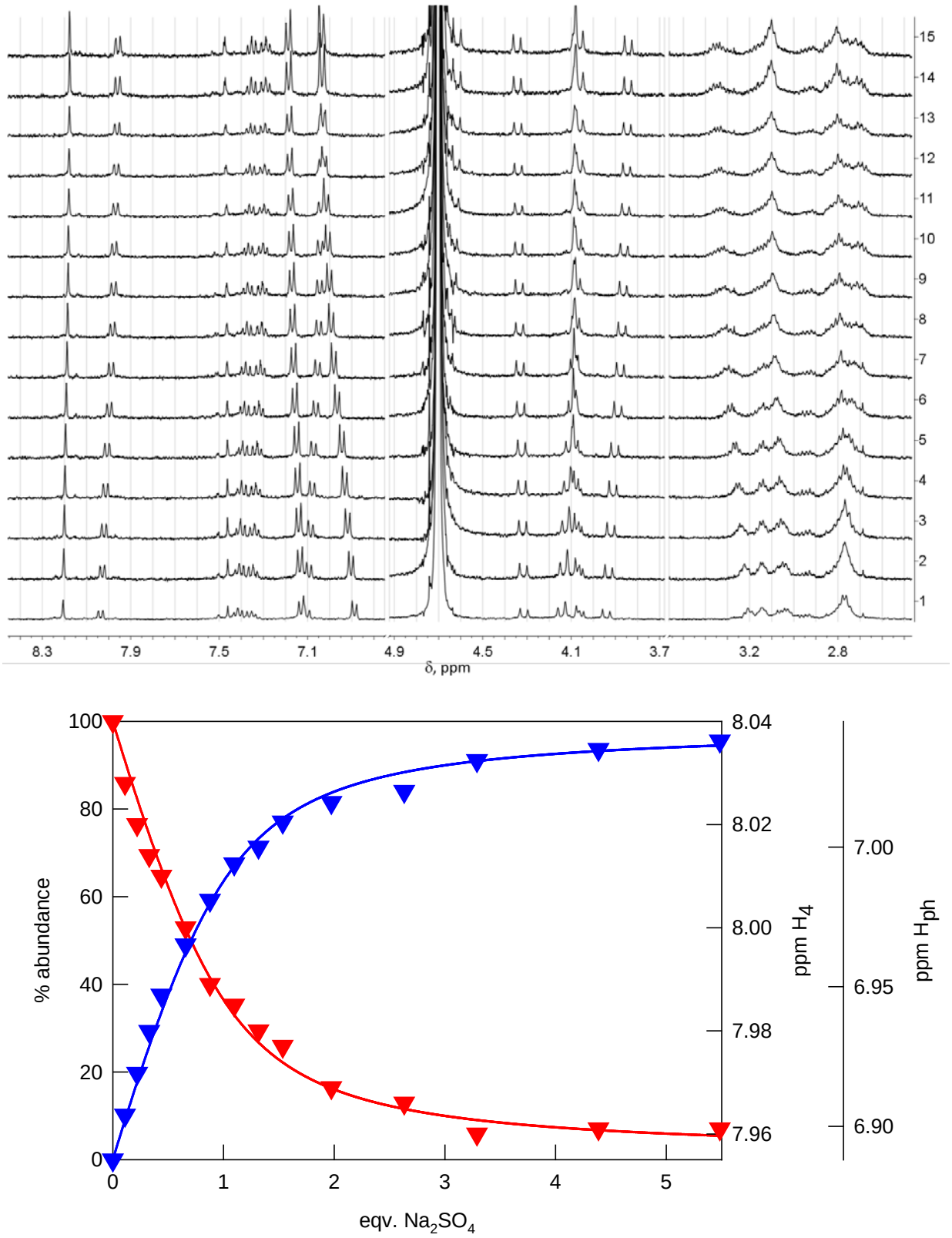

Figure S18. top: family of ^{1}H-NMR spectra taken over the course of the titration of $[\mathbf{1}H_6]^{6+}$ (0.6 mM) in D_2O (pD = 2, CF_3SO_3Na 0.05M) with a standard solution of Na_2SO_4, spectrum 1 corresponds to the free receptor; bottom: experimental profiles (chemical shifts of H_{ph} and H_4: blue and red symbols, respectively) superimposed to the distribution diagram of the species vs. equivalents of the added sodium salt. red line = % free $[\mathbf{1}H_6]^{6+}$, blue line = % $[\mathbf{1}H_6(SO_4)]^{4+}$

8. Spectrofluorimetric titrations

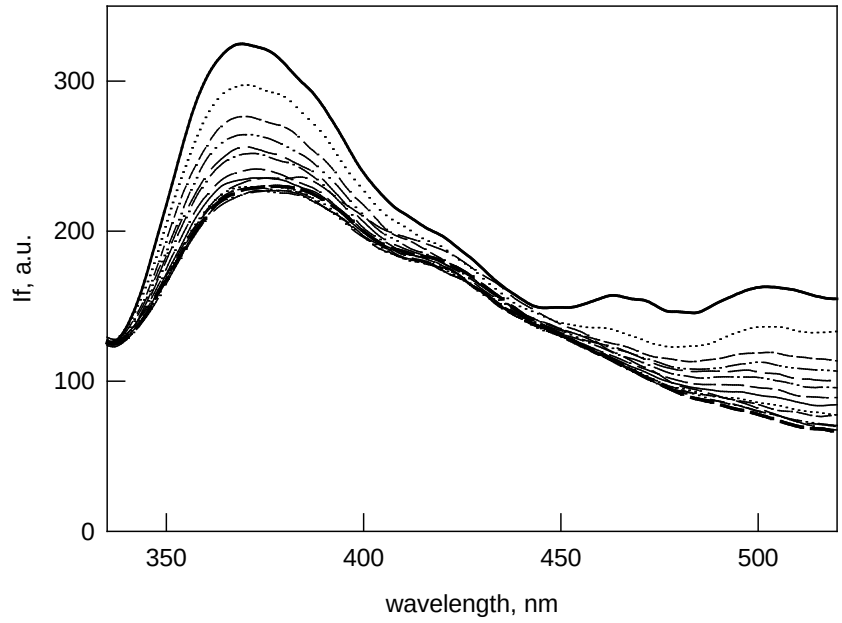

Figure S19. Emission spectra (Intensity in arbitrary units *vs.* wavelength) recorded over the spectrofluorimetric titration of an aqueous solution of $[\mathbf{1}H_6]^{6+}$ (5 μM, λ_{exc} = 284 nm) with $NaReO_4$ at pH=2. Solid and dashed lines: initial and final spectra, respectively.

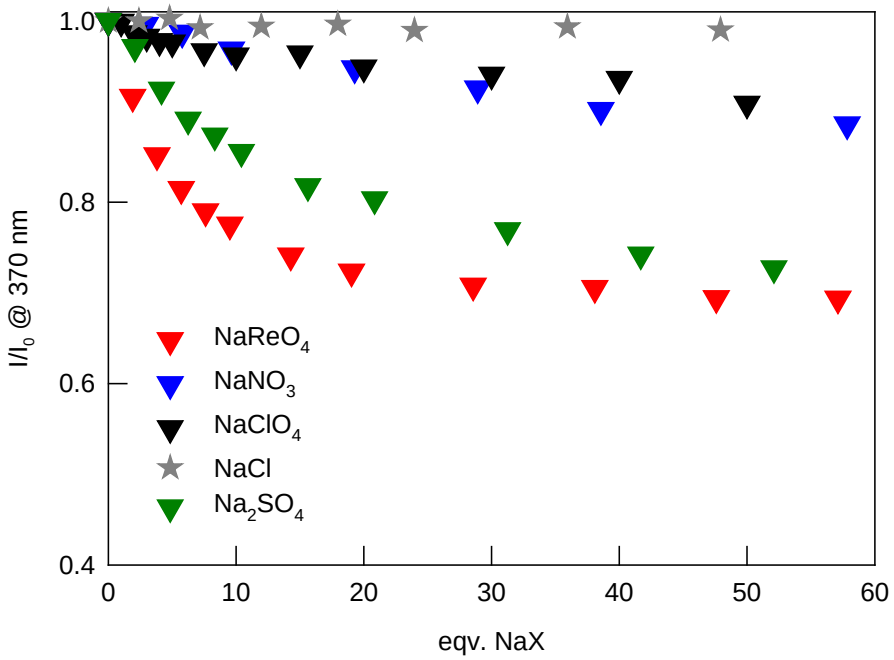

Figure S20. The experimental profiles are relative to spectrofluorimetric titrations on $[\mathbf{1}H_6]^{6+}$ (5 μM in 0.05M CF_3SO_3Na, λ_{exc} = 284 nm) with various sodium salts. Profiles of the normalized intensity (I/I_0) at 370 nm *vs.* equivalents of the added NaX. The titrant solutions were prepared in the same solvent medium as that used for the receptor.

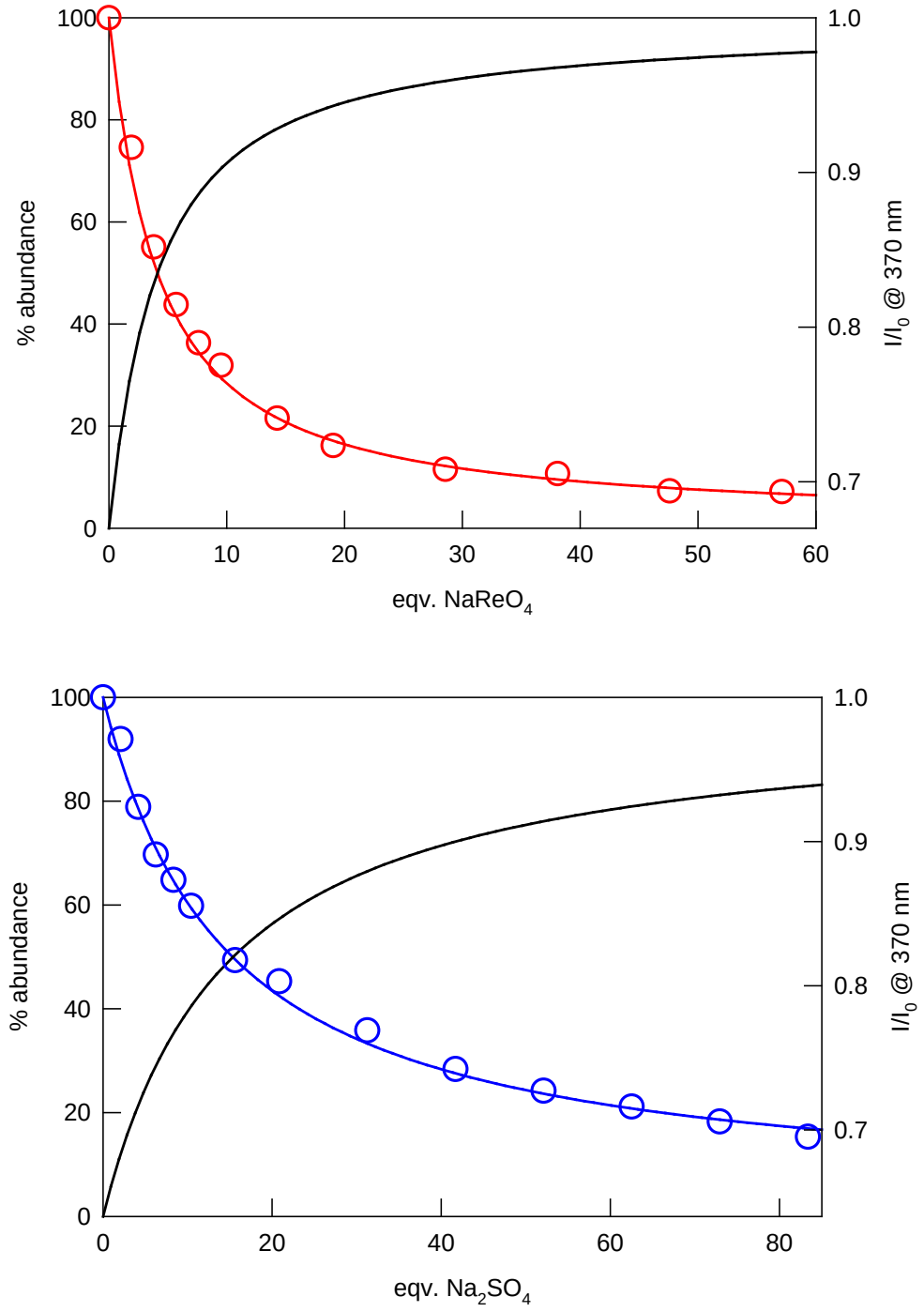

Figure S21. Profiles of the normalized intensity (I/I_0 at 370 nm) *vs.* equivalents of the added NaX, obtained from the spectrofluorimetric titrations of the $[\mathbf{1}H_6]^{6+}$ receptor (5 μM in 0.05M CF_3SO_3Na, λ_{exc} = 284 nm) with the chosen sodium salt (top and bottom figures: $NaReO_4$ and Na_2SO_4, respectively). Experimental profiles are superimposed to the distribution diagrams calculated for $\log K_{11}$ = 4.70 (top, $NaReO_4$) and 4.21 (bottom, Na_2SO_4).

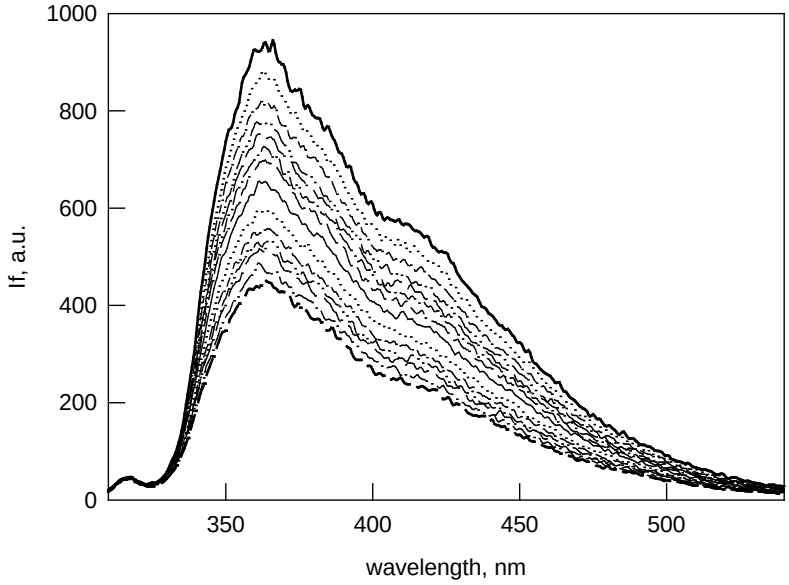

Figure S22. Emission spectra (Intensity in arbitrary units *vs.* wavelength) recorded over the spectrofluorimetric titration of an aqueous solution of $[\mathbf{2}H_6]^{6+}$ (5 μM, λ_{exc} = 284 nm) with $NaReO_4$ at pH = 2. Solid and dashed lines: initial and final spectra, respectively.

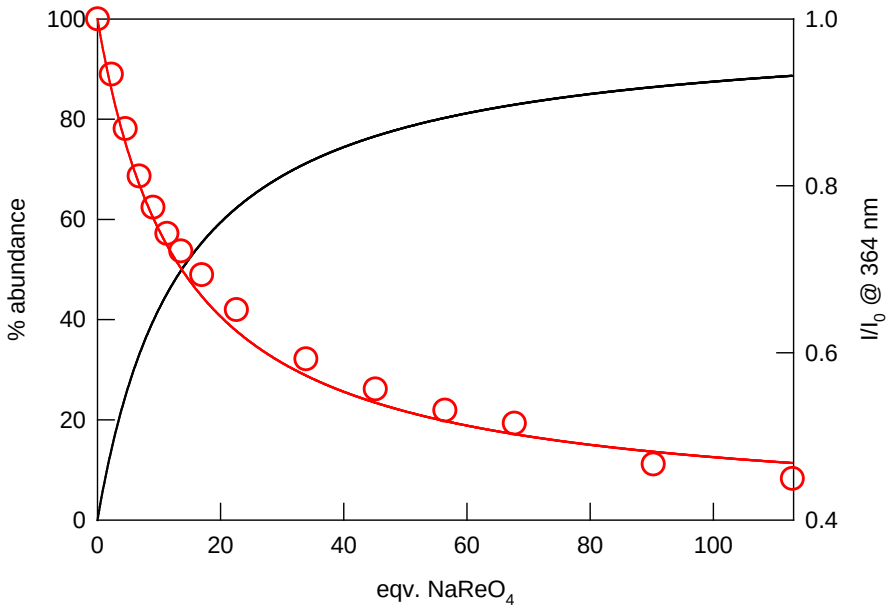

Figure S23. Profile of the normalized intensity (I/I_0 at 364 nm) *vs.* equivalents of the added NaX, obtained from the spectrofluorimetric titrations of $[\mathbf{2}H_6]^{6+}$ (5 μM, pH 2, λ_{exc} = 284 nm) with $NaReO_4$. The experimental profile is superimposed to the distribution diagrams calculated for $\log K_{11}$ = 4.19.

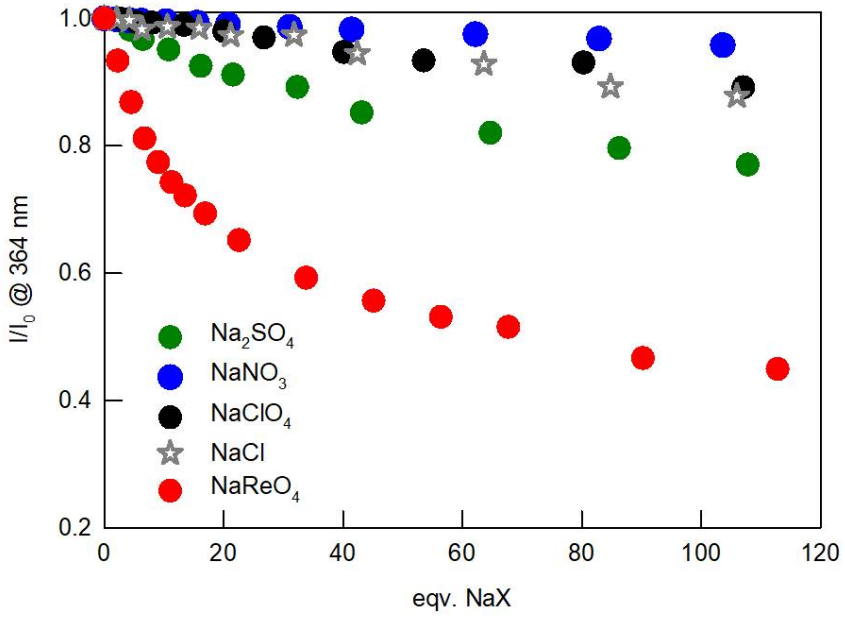

Figure S24. Profiles of the normalized intensity (I/I_0) at 364 nm *vs.* equivalents of the added NaX, relative to the spectrofluorimetric titrations of $[\mathbf{2}H_6]^{6+}$ (5 μM, pH 2, λ_{exc} = 284 nm) with various sodium salts.

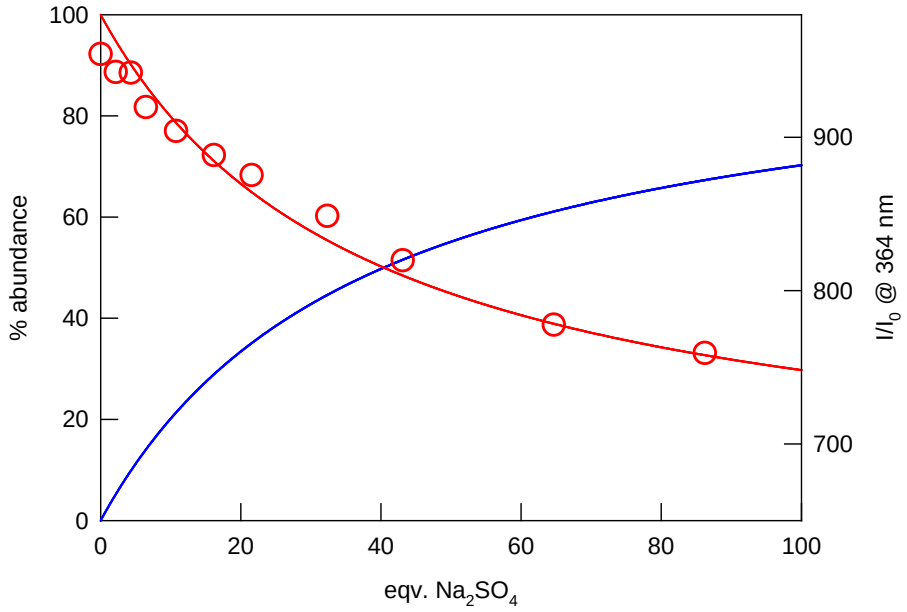

Figure S25. Profile of the normalized intensity (I/I_0 at 364 nm) *vs.* equivalents of the added NaX, obtained from the spectrofluorimetric titrations of $[\mathbf{2}H_6]^{6+}$ (5 μM, pH 2, λ_{exc} = 284 nm) with Na_2SO_4. The experimental profile is superimposed to the distribution diagrams calculated for $\log K_{11}$ = 3.72.

9. CD studies in complex matrices

Commercial fruit pineapple-lime juice was diluted (10×) and acidified with aqueous CF_3SO_3H until pH 2. The obtained solution was employed as solvent mixture for the preparation of standard solutions of both the receptor and sodium perrhenate. On the other hand, AUM was prepared by dissolving the components reported in Table S2 in demineralized water.[S7] The obtained solution was diluted (30×) and acidified with aqueous CF_3SO_3H until pH 2. The final mixture was employed in the preparation of the samples for CD titrations experiments. We remark that the concentration of the $[\mathbf{1}H_6]^{6+}$ (0.05 mM), employed in the titration experiment, was much lower than the concentrations of chloride, nitrate and sulfate in solution (~ 3 mM, 0.2 mM and 0.4 mM, respectively). The pH value was checked before and after titrations.

Table S2: Components of AUM dissolved in demineralized water.

Component	**Concentration**	**after dilution 30x**
Citric acid	2 mM	$6.7\ 10^{-5}$ M
Sodium chloride	90 mM	3 mM
L-glutamine	2 mM	$6.7\ 10^{-5}$ M
Urea	170 mM	5.7 mM
Creatinine	7 mM	$2.3\ 10^{-4}$ M
Calcium chloride.$2H_2O$	0.25 mM	$8.3\ 10^{-6}$ M
Magnesium sulphate.$7H_2O$	2 mM	$6.7\ 10^{-5}$ M
Sodium sulphate.$10H_2O$	10 mM	$3.3\ 10^{-4}$ M
Sodium nitrate	6 mM	$2\ 10^{-4}$ M
Potassium dihydrogen phosphate	1.8 mM	$6\ 10^{-5}$ M

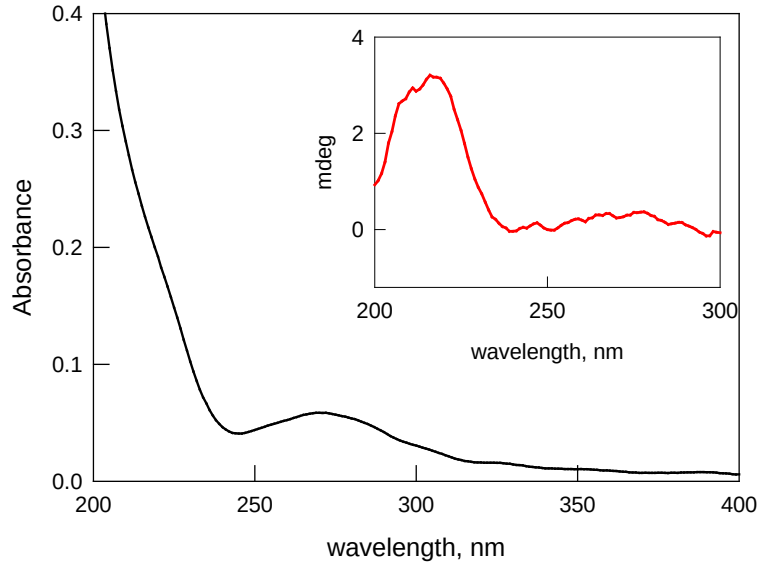

Figure S26: UV-vis and CD spectra (black and red lines, respectively) of commercial pineapple-lime juice after 10× dilution with demineralized water. The solution pH was brought to 2 by addition of aqueous CF_3SO_3H.

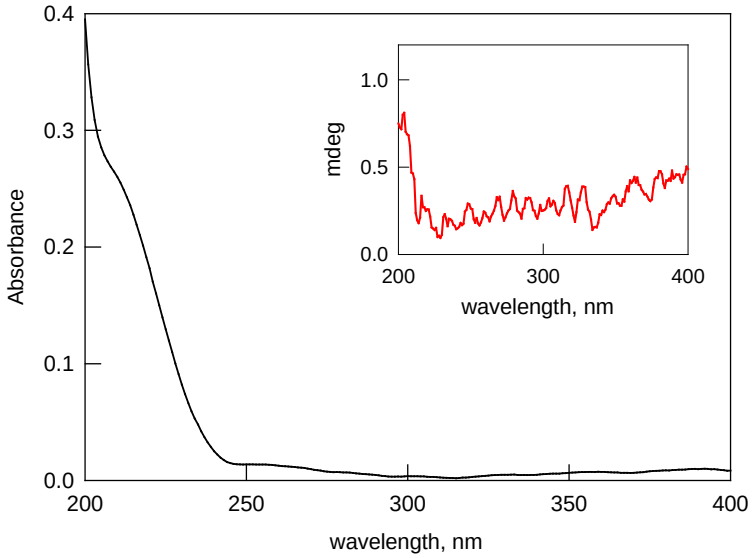

Figure S27: UV-vis and CD spectra (line and red lines, respectively) of AUM after 30× dilution with demineralized water. The solution pH was brought to 2 by addition of aqueous CF_3SO_3H.

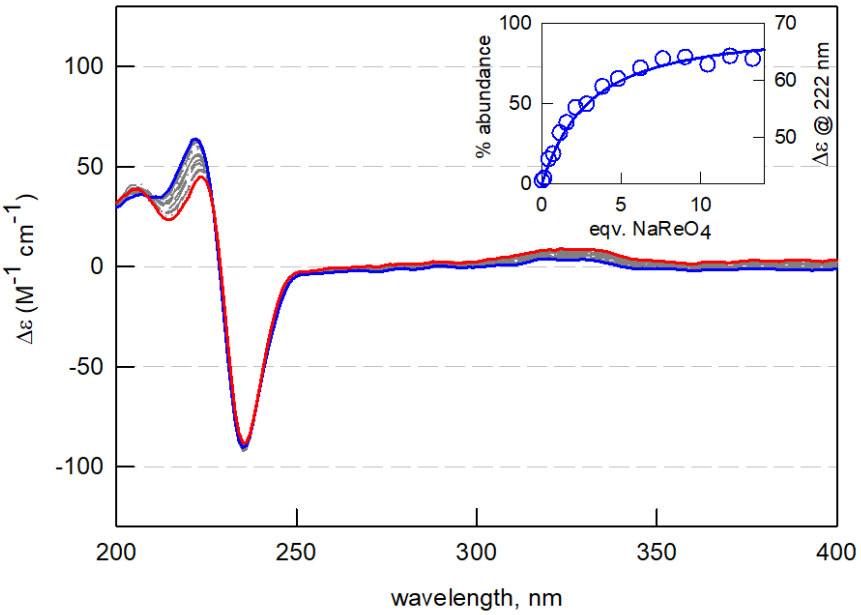

Figure S28: CD spectra taken over titration of $[\mathbf{1}H_6]^{6+}$ (0.05 mM) with $NaReO_4$ in diluted (30×) AUM at pH 2; red and blue lines: initial and final spectra, respectively. Inset: % $[\mathbf{1}H_6(ReO_4)]^{5+}$ *vs.* eqv. $NaReO_4$ (blue line), calculated for $\log K_{11} = 3.93(2)$, superimposed to the experimental profile (circles).

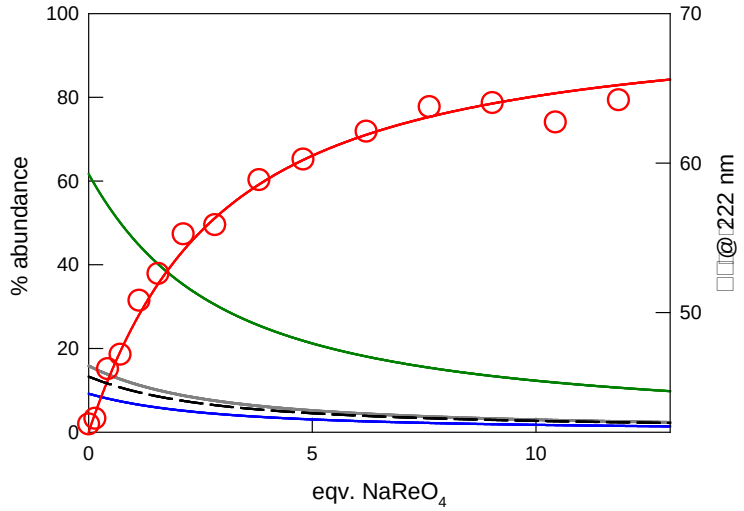

Figure S29. Distribution diagram of the species in solution over the course of the CD titration of $[\mathbf{1}H_6]^{6+}$ (50 μM) with $NaReO_4$ in diluted AUM; red line: % $[\mathbf{1}H_6(ReO_4)]^{5+}$; green line: % $[\mathbf{1}H_6(SO_4)]^{4+}$; grey line: % $[\mathbf{1}H_6(Cl)]^{5+}$; black dashed line: % *free* $[\mathbf{1}H_6]^{6+}$, blue line: % $[\mathbf{1}H_6(NO_3)]^{5+}$, red symbols: experimental titration profile of Δε at 222 nm vs. equivalents $NaReO_4$. Solutions were prepared in (30×) diluted AUM, taken to pH 2 with aqueous CF_3SO_3H. The diagram was built using the Hyss software (Hyperquad package). In particular, knowing the concentration of the potential interfering anions and the binding constants in aqueous solution at pH 2 (reported in Table 1), we could estimate that $[\mathbf{1}H_6]^{6+}$ is initially distributed in AUM among the following forms: 62%, $[\mathbf{1}H_6(SO_4)]^{4+}$; 16%, $[\mathbf{1}H_6(Cl)]^{5+}$; 13%, *free* $[\mathbf{1}H_6]^{6+}$; 9%, $[\mathbf{1}H_6(NO_3)]^{5+}$ (where % corresponds to the molar fraction × 100).

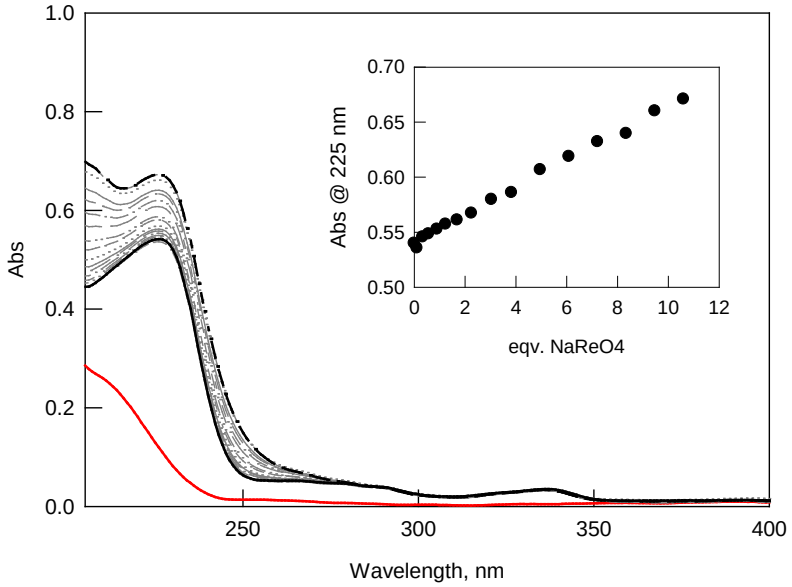

Figure S30: UV-vis. spectra taken over titration of $[\mathbf{1}H_6]^{6+}$ (0.05 mM) with $NaReO_4$ in diluted (30×) AUM at pH 2 (solid and dashed black lines: initial and finale spectra, respectively); red line: spectrum of diluted AUM. Inset graph: profile of absorbance at 225 nm *vs.* equivalents of the added $NaReO_4$.

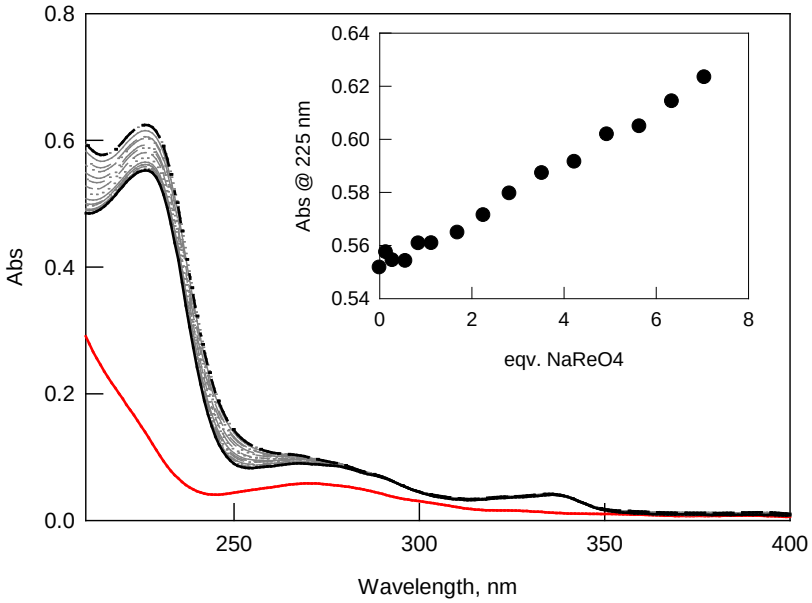

Figure S31: UV-vis. spectra taken over titration of $[\mathbf{1}H_6]^{6+}$ (0.05 mM) with $NaReO_4$ in diluted (10×) fruit juice at pH 2 (solid and dashed black lines: initial and finale spectra, respectively); red line: spectrum of the diluted juice. Inset graph: profile of absorbance at 225 nm *vs.* equivalents of the added $NaReO_4$.

10. Copies of NMR and Mass spectra of New Compounds

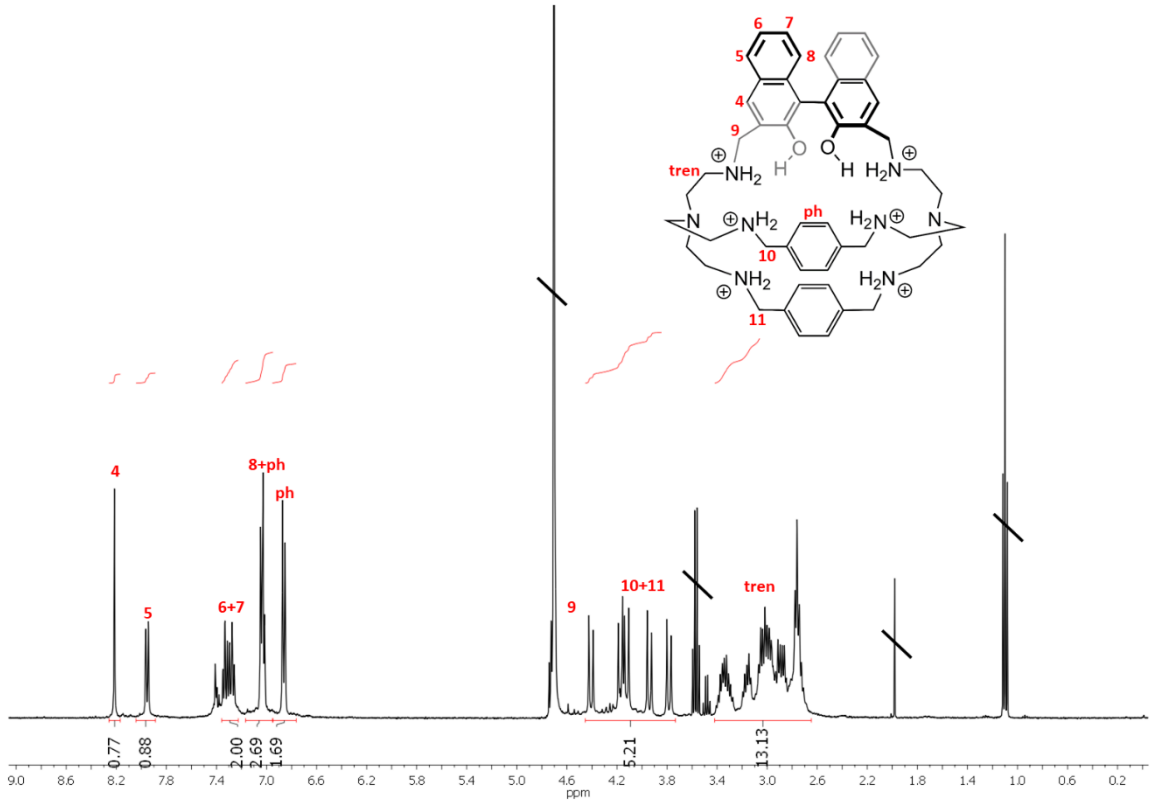

Figure S32. ^{1}H-NMR spectrum of **1** (400 MHz) in D_2O (+ excess CF_3SO_3H).

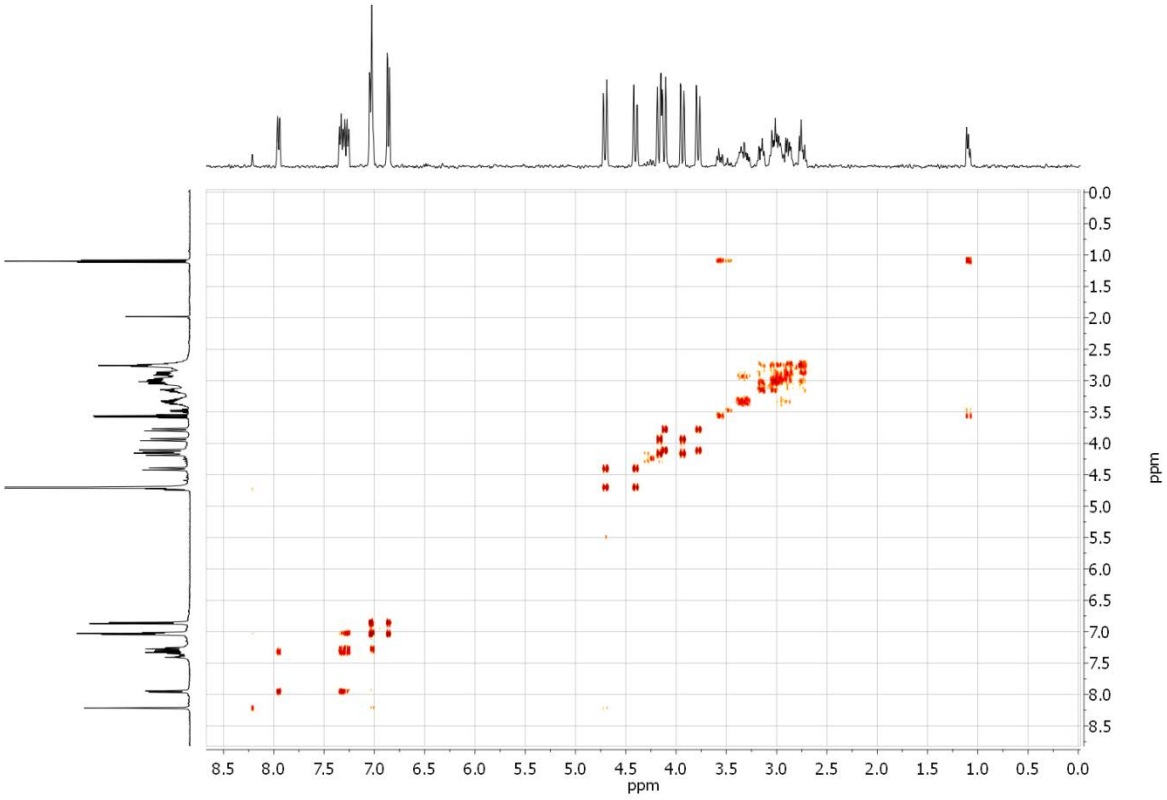

Figure S33. COSY spectrum of **1** (400 MHz) in D_2O (+ excess CF_3SO_3H).

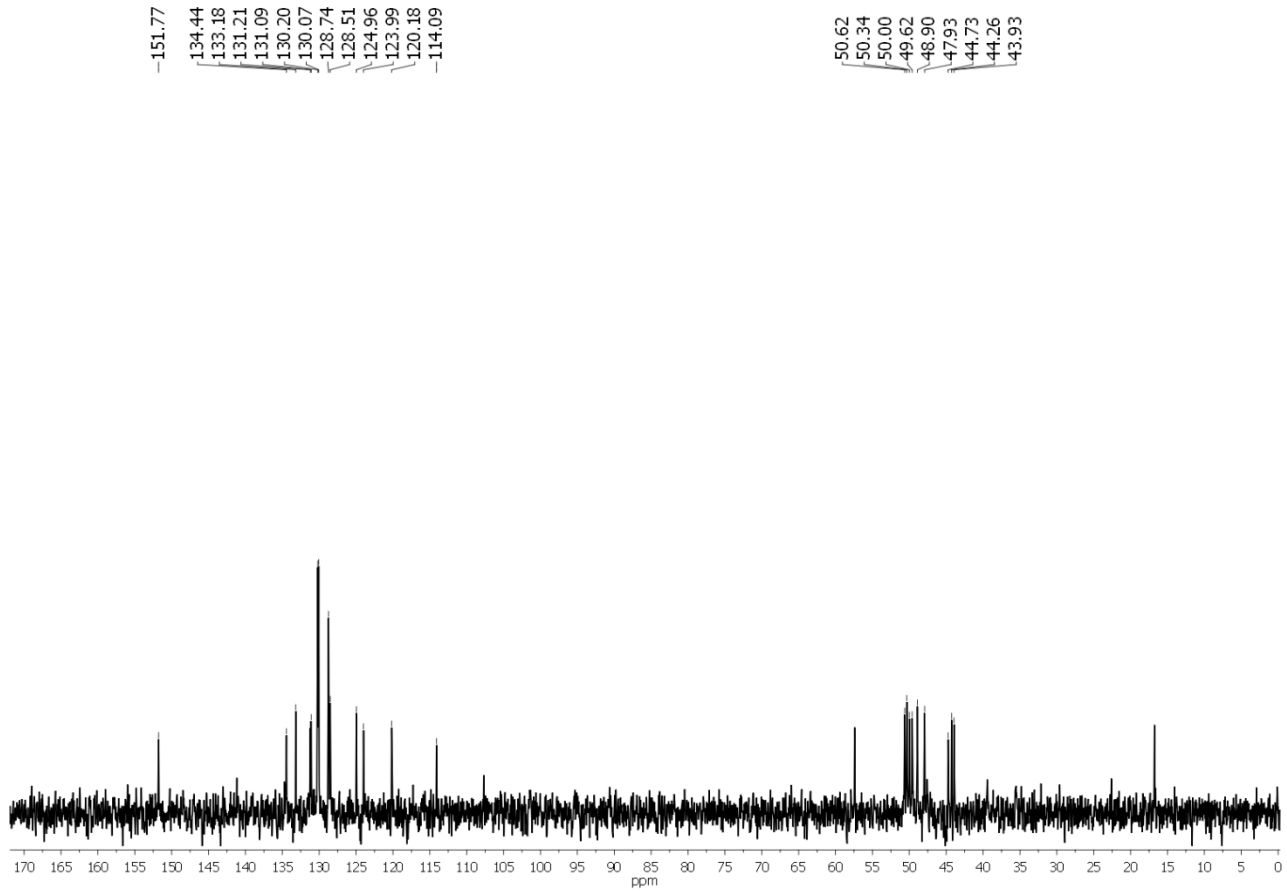

Figure S34. ^{13}C-NMR spectrum of **1** (100 MHz) in D_2O (+ excess CF_3SO_3H).

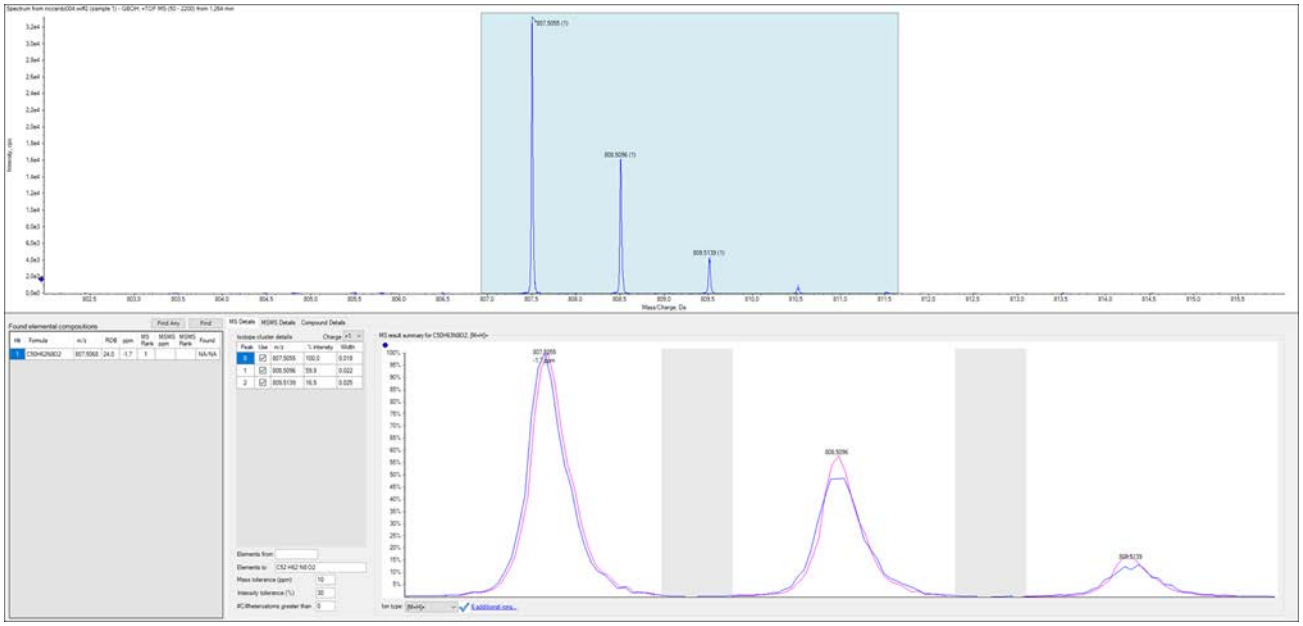

Figure S35. HRMS-ESI of [**1**+H^+]$^+$ in CH_3CN. Up: zoom scan of the peak at 807.5055 m/z obtained from the experimental HRMS-ESI spectrum. Bottom: calculated spectrum of the adduct [**1**+H^+]$^+$ superimposed to the experimental one.

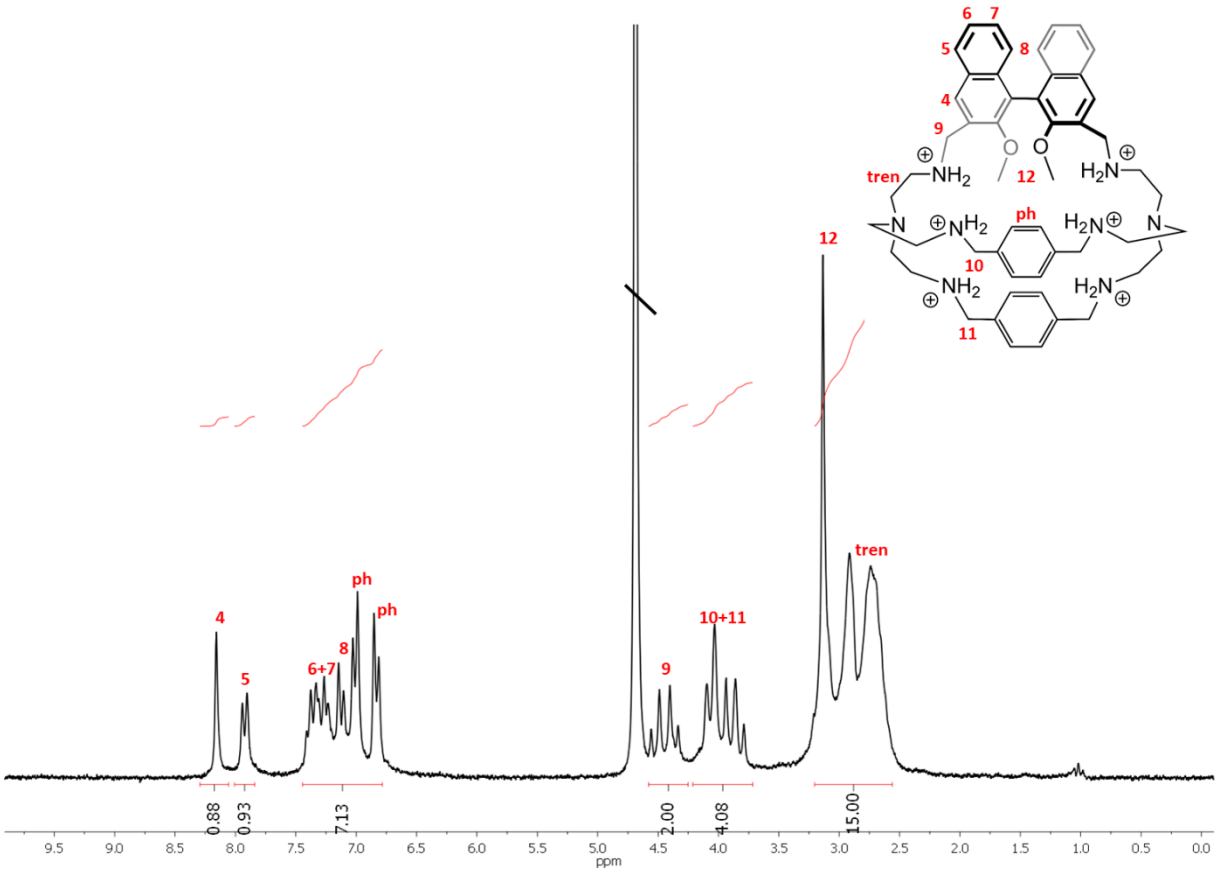

Figure S36. ^{1}H-NMR spectrum of **2** (300 MHz) in D_2O (+ excess CF_3SO_3H).

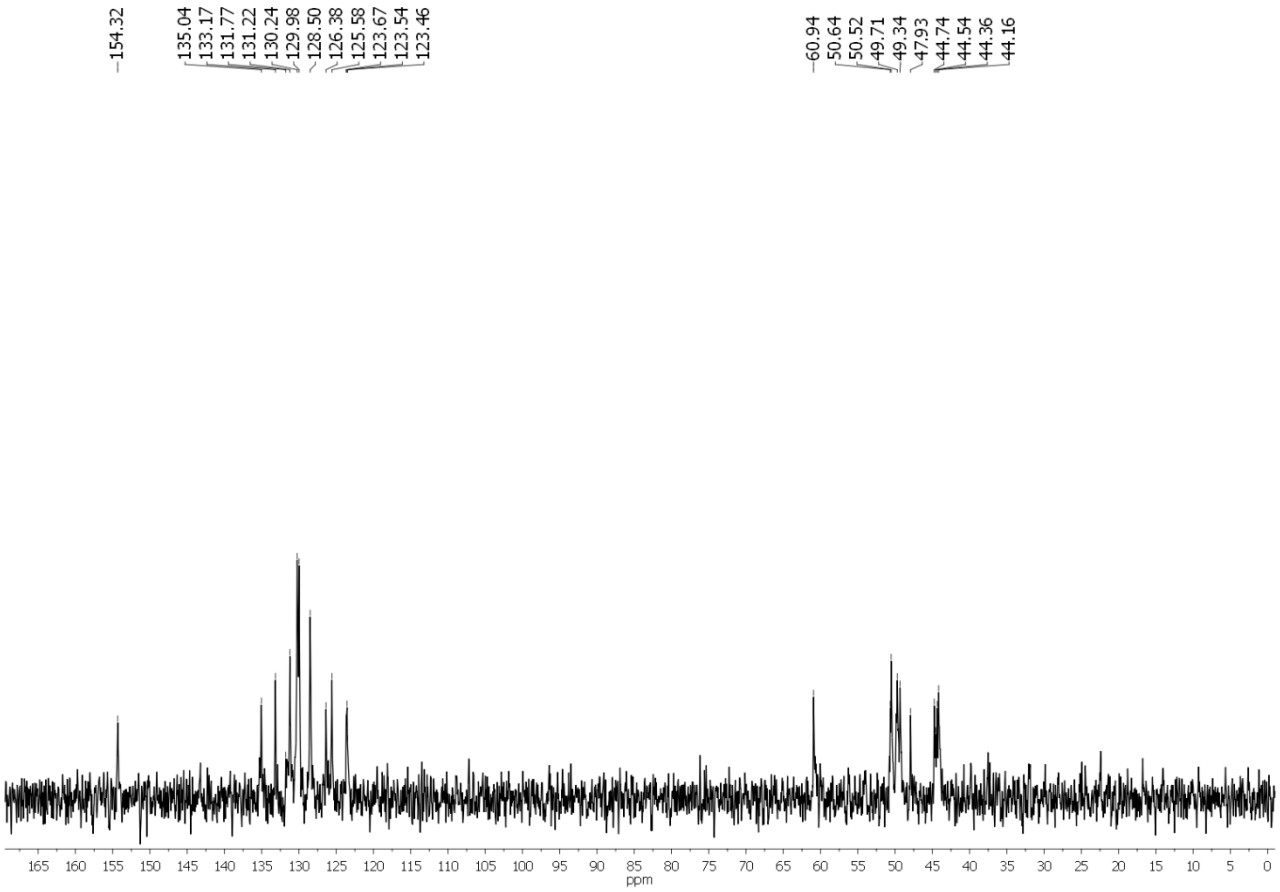

Figure S37. ^{13}C-NMR spectrum of **2** (100 MHz) in D_2O (+ excess CF_3SO_3H).

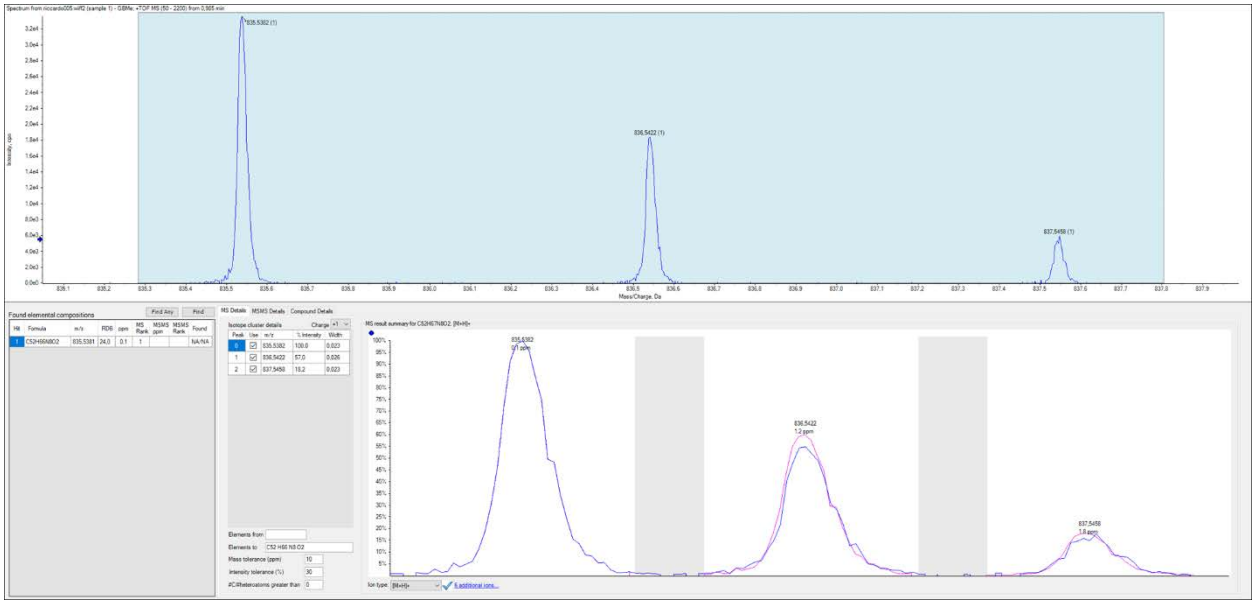

Figure S38. HRMS-ESI of [**2**+H$^+$]$^+$ in CH_3CN. Up: zoom scan of the peak at 835.5382 m/z obtained from the experimental HRMS-ESI spectrum. Bottom: calculated spectrum of the adduct [**2**+H$^+$]$^+$ superimposed to the experimental one.

References

[S1] V. Amendola, G. Bergamaschi, M. Boiocchi, R. Alberto and H. Braband, *Chem. Sci.*, 2014, **5**, 1820-1826.

[S2] A. Thevenet, A. Miljkovic, S. La Cognata, C. Marie, C. Tamain, N. Boubals, C. Mangano, V. Amendola and P. Guilbaud, *Dalton Trans*., 2021, **50**, 1620-1630.

[S3] Y. Zhou, D. Zhang, Y. Zhang, Y. Tang and D. Zhu, *J. Org. Chem*., 2005, **70**, 6164-6170.

[S4] M. J. Frisch, G. W. Trucks, H. B.Schlegel, G. E. Scuseria *et al*. Gaussian 09, Revision B.01; Gaussian, Inc., Wallingford, CT, 2010.

[S5] P. Gans, A. Sabatini and A. Vacca, *Talanta*, 1996, **43**, 1739-1753.

[S6] S. La Cognata, R. Mobili, F. Merlo, A. Speltini, M. Boiocchi, T. Recca, L. J. Maher III and V. Amendola, *ACS Omega*, 2020, **5**, 26573-26582

[S7] T. Brooks and C. W. Keevil, *Lett. Appl. Microbiol.*, 1997, **24**, 203-206.